DEVELOPMENT OF POROUS LIGHTWEIGHT AGGREGATES FOR CONTROLLED NUTRIENT RELEASE IN PLANT FERTILIZATION

PANADDA RUNGRUENG

A THESIS SUBMITTED IN PARTIAL FULFILLMENT OF THE REQUIREMENT FOR
THE DEGREE OF MASTER OF SCIENCE IN APPLIED PHYSICS
DEPARTMENT OF PHYSICS SCHOOL OF SCIENCE
KING MONGKUT'S INSTITUTE OF TECHNOLOGY LADKRABANG
2025

KMITL-2025-SC-M-030-049

Thesis Title	Development of Porous Lightweight Aggregates for Controlled Nutrient Release in Plant Fertilization
Student Name	Panadda Rungrueng
Student ID	65056056
Degree	Master of Science (Applied Physics)
Department	Physics
Year	2025
Thesis Advisor	Assist.Prof. Dr. Mettaya Kitiwan

Abstract

This research focuses on the development of lightweight aggregates (LWAs) as a planting material with integrated fertilizer functionality for indoor horticultural applications. The primary objective was to optimize the fabrication process of clay-based LWAs incorporating expanded perlite (EP) and to identify effective absorbing media for fertilizer incorporation. This dual-purpose material aims to improve soil aeration and water retention while gradually supplying essential nutrients to plants.

The first part of the study involved investigating the effects of EP content and sintering temperature on the physical properties of LWAs. Raw red clay was mixed with EP at varying proportions (0–40 wt.%) and sintered at 800°C, 900°C, and 1000°C. The physical characteristics of the sintered pellets such as bulk density, porosity, and water absorption were measured using the Archimedes method. Results showed that increasing EP content significantly reduced bulk density while enhancing porosity and water absorption. Optimal structural performance was observed at 20–30 wt.% EP content sintered at 900°C, yielding lightweight and highly porous aggregates suitable for planting applications.

In the second part, fertilizer (NPK 16-16-16) was incorporated into sintered EP-LWAs using a vacuum-assisted infiltration technique. Three types of absorbing media such as carboxymethyl cellulose (CMC), glycerol, and vegetable oil were evaluated for their ability to carry and retain fertilizer nutrients. CMC exhibited the most favorable properties, forming a stable gel with the fertilizer and achieving the highest nutrient loading: 1.3% nitrogen (N), 1.1% phosphorus (P), and 1.4% potassium (K). In contrast,

glycerol and vegetable oil resulted in phase separation and poor nutrient entrapment, making them unsuitable as fertilizer carriers. Elemental distribution analysis using energy-dispersive X-ray spectroscopy (EDS) confirmed the homogeneous dispersion of potassium and phosphorus throughout the LWA microstructure, verifying the successful incorporation of fertilizer into the porous framework. Nitrogen detection was limited due to instrumental sensitivity to low atomic number elements. Preliminary release testing of the optimized EP LWAs loaded with 50 wt.% fertilizer (EP LWAs-F50) revealed a biphasic release profile. A rapid initial release phase was observed, with approximately 78.5% of the nutrient content released within the first 24 h. and complete release achieved at 168 h. Therefore, the current formulation cannot yet be classified as a slow-release system.

In summary, this study successfully demonstrates the feasibility of fabricating EP-enhanced LWAs with integrated fertilizer using CMC as the absorbing medium. The resulting material is lightweight, porous, and nutrient-rich, making it highly suitable for decorative plant cultivation and urban gardening. This development offers a sustainable alternative to conventional fertilizer systems and contributes to the growing demand for eco-friendly horticultural solutions.

Keywords: Lightweight Aggregate (LWA), Expanded Perlite, Fertilizer, Carboxymethyl Cellulose (CMC), Porous Planting Material

Acknowledgements

The generosity and support of many people made this thesis possible. I would like to sincerely thank each and every one of you in the described below:

First of all, I would like to deepest thank my advisor, Asst. Prof. Dr. Mettaya Kitiwan, as well as Dr. Nittaya Keawprak, and Asst. Prof. Dr. Keerayoot Srinuanjan for their advice, encouragement, and support for everything in the research process.

A special thanks to my colleagues and friends. They offered help during the hard times and also made this thesis more enjoyable.

Finally, I would like to thank my family for their support and understanding during the thesis process ever is a long and hard journey.

This thesis would not been possible without the combined of them. Thank you all for being an important part of this Thesis.

Ms. Panadda Rungrueng

Table of contents

List of tables

List of figures

Chapter 1

Introduction

1.1 Research motivation

In recent times, the trend of decorating homes with indoor plants has become more popular. The benefits of indoor plants have been well-documented, with studies showing that they can improve air quality, reduce stress levels, boost productivity, and enhance overall well-being. The COVID-19 pandemic has resulted in a significant shift towards work-from-home or self-quarantine, leading to an increased demand for greenery as people seek to bring nature indoors and improve their living environment. As a result of this growing trend, there has been a surge in the market for indoor gardening products and accessories, such as planting materials, fertilizers, and planters.

Lightweight aggregate (LWA), a highly porous planting material, has emerged as a particularly interesting option due to their ability to enhance soil transparency and promote water absorption for plants while also providing adequate sufficient oxygen for their roots. Although commercial LWAs are a commonly used planting material, they do not contain any plant nutrients and are primarily used for support or decorative purposes. To utilize them for enhancing plant growth, it is essential to supplement LWA with fertilizers to ensure a sufficient supply of nutrients for the plants.

This research is focused on the development of LWA with integrated fertilizer components. The LWA are designed to incorporate fertilizer through absorbing media that allows for the slow release of nutrients to plants over an extended duration. One common problem encountered when using chemical fertilizers is that the nutrients are rapidly released upon watering, potentially leading to an overabundance of nutrients in the soil and water sources. Slow-release fertilizers, typically consisting of chemical fertilizers coated in a specialized polymer, have been developed to address this issue by gradually and consistently dissolving through the coating layer over an extended duration. This approach ensures that plants receive sufficient nutrients over an extended period, without negatively impacting on the surrounding environment. Incorporating slow-release fertilizer into LWA provides added convenience as it delivers sufficient nutrients to the soil while simultaneously enhancing its aeration properties. However, there has been a lack of research and development concerning such planting materials.

The research project is divided into two main parts. The first part focuses on studying the formation conditions of the green LWA, including the clay mixing ratio (clay, perlite, and binder), the sintering temperature (800–1000°C). The aim is to establish the optimal conditions that result in LWA with the appropriate bulk density, porosity, and water absorption. In the second part, the addition of fertilizers to the LWA is investigated. This section also involves investigating suitable absorbing media and methods for incorporating the fertilizers into the clay balls. The preliminary examination of fertilizer release rate is also conducted.

The findings of this research project will contribute to the development of a novel planting material - LWA integrated with fertilizer. This innovation will have significant applications in agriculture, particularly in the cultivation of indoor decorating plants. The incorporation of fertilizers within the LWA will enhance plant growth by improving soil aeration and nutrient supply. Additionally, the proposed material could have applications in agricultural production.

1.2 Objectives of the study

1) To investigate the optimal mixing ratio and sintering conditions for producing LWA by analyzing various properties, including bulk density, porosity, and water absorption.
2) To develop a method for incorporating fertilizers into LWA and investigate the nutrient release behavior.

1.3 Scope(s) of the study

1) Theoretical study and literature review of clay balls as planting materials and slow-released fertilizers mechanism.
2) Determination of the optimal mixing ratio of clay and perlite, with perlite ranging from 10-40 % by weight and investigation of the appropriate sintering process, with the temperature ranging from 800-1000°C.
3) Investigation of suitable absorbing media and methods for incorporating fertilizers into sintered clay balls.

1.4 Benefits of the study

1) Acquire knowledge and comprehension of the theory and principles behind producing LWA mixed with perlite for use as planting materials.
2) Determine the optimal conditions for producing clay balls mixed with perlite, including the appropriate mixing ratio and sintering temperature.
3) Identify the most effective method for incorporating fertilizers into sintered clay balls for slow-release nutrient delivery to plants.

Chapter 2

Theory and literature reviews

2.1 Lightweight expanded clay aggregate (LECA)

Lightweight expanded clay aggregate, or LECA, is a type of lightweight aggregate (LWA) that is produced by heating clay pellet in a kiln at temperatures of 800°C or higher [1]. The firing process increases the porosity of aggregate and results in an interconnected pore structure with different pore size as shown in Figure 2.1 [2]. LECA is extensively produced in many countries and marketed under various product names. Some countries, including the UK, Iran, Portugal, Finland, Germany, Italy, Denmark, and Switzerland, use the term "leca" to brand their LECA products. On the other hand, Sweden, China, Poland, and Russia brand it as "Keramzite." In Spain, it is known as "liapour," while in South Africa, it is marketed as "Argex." These different names reflect the regional variations in branding for LECA across different countries [3].

During the manufacturing process, clay undergoes expansion, leading to the development of distinct internal structures. As the clay is heated, gas is released within the pellets, which become trapped during the subsequent cooling process. The combustion of organic compounds contributes to the expansion of clay, resulting in the formation of porous and lightweight clay pellets that can expand up to 5-6 times their original volume [4].

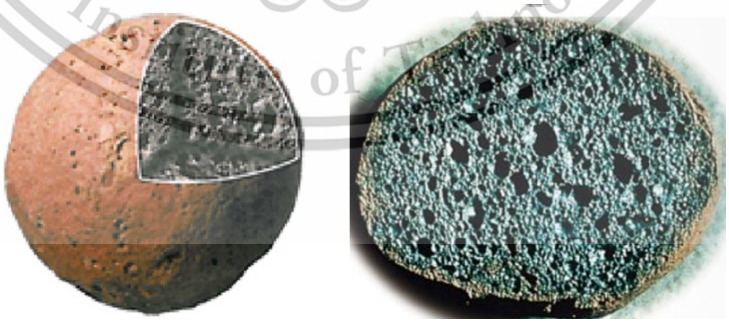

Figure. 2.1 The cross sectional of LECA, demonstrating the interconnected pore structure with different pore sizes [2].

LECA exhibits a range of colors, including dark brown, reddish, and reddish-brown, influenced by factors such as the chemical composition and the specific production process employed. It is typically manufactured without the use of hazardous materials, possesses a natural pH value, is non-flammable, and exhibits non-biodegrade properties. The size of LECA can vary and depends on the manufacturer, as they offer a range of options including built-in LECAs in different sizes. The unique characteristics of LECA products, such as density, weight, and diameter, can vary depending on the application requirements [2]. Additionally, clay is the primary raw material used in LECA production, which can be blended with various additives such as shale, petite, granite, and quarry waste. Furthermore, industrial by-products like fly ash, sewage sludge, and contaminated soil can also be incorporated into the production process of LECA [5].

LECA is indeed a versatile material with a wide range of applications. It can be used as a lightweight aggregate in construction for producing blocks and precast concrete. It is also used as a lightweight fill material in geotechnical applications, providing a stable and porous base for structures. In the production of lightweight concrete, LECA is commonly used as an aggregate and can provide thermal insulation properties [2]. The porous structure of LECA makes it useful as an absorbent for the removal of pollutants from water. LECA has shown the potential to remove heavy metal such as Pb, Cu, and Cd from industrial wastewater [6]. Moreover, it has been shown to effectively remove many pollutants present in agricultural wastewater, making it an eco-friendly option for treating agricultural wastewater [6]. Additionally, LECA can drain groundwater and surface water to regulate groundwater pressure [7]. LECA has good water absorption properties with strong and durable structure and does not react with nutrients. As a result, it is highly suitable for use as a planting material, providing efficient drainage and aeration capabilities.

Table 2.1 shows the chemical composition of LECA characterized using X-ray fluorescence (XRF) analysis. The composition of LECA produced from different sources of clay has generally dominated by 5–6 main components, including 60–70% SiO_2, 15–18% Al_2O_3, 4–7% Fe_2O_3, 1–4% MgO, CaO, Na_2O, and other minor constituents contributing less than 1%.

Table 2.1 The chemical composition of LECA is produced from natural clay and marine clay mixed with industrial sludge.

Chemical composition	Sharifnia et al. (2016) [8]	Kalhori et al. (2013) [9]	Laursen et al. (2006) [10]
	100% clay	100% clay	90% marine clay + 10% industrial sludge
SiO_2	64.83	61.67	70.7
Al_2O	15.05	18.51	15.3
Fe_2O_3	7.45	6.014	4.5
MgO	3.67	3.97	1.02
CaO	2.98	3.5	3.8
K_2O	2.55	3.28	1.39
Na_2O	1.1	1.54	0.51
TiO_2	0.63	0.65	0.57
SO_3	0.11	0.23	1.5
P_2O_5	0.13	0.19	nd*
SrO	-	0.13	0.026
Cl-	-	-	0.13
MnO	0.13	-	0.03
CuO	-	-	0.021
F	-	-	Nd
ZnO	-	-	0.015
ZrO_2	-	-	0.101
BaO	-	-	0.36

*nd = No data

2.2 Slow-release fertilizer

2.2.1 The significance of slow-release fertilizer

The agricultural industry offers a wide range of commercial fertilizers. Quick-release fertilizers (QRFs) have been commonly used as they readily dissolve in water and provide nutrients to plants soon after being applied to the soil. However, they release all the available nutrients quickly, without synchronizing with the dynamic growth needs of crops. To address these challenges, the fertilizer industry has been focused on developing efficient fertilizers known as slow-release fertilizers (SRFs) and

controlled-release fertilizers (CRFs). These innovative fertilizers are designed to contain nutrients that are not immediately available for absorption by plants. Instead, they are released gradually over time, minimizing the problems associated with rapid nutrient release and loss. The use of SRFs and CRFs represents an effective approach to ensure a reliable and consistent nutrient supply for crops throughout their growth cycle [11].

2.2.2 Definition of slow-release fertilizer

Slow-release fertilizer refers to a type of fertilizer that is formulated with plant nutrients in a readily absorbable form, which allows for gradual and prolonged release of these nutrients to plants. According to the European Standardization Committee (CEN) [12], slow-release fertilizers are defined as follows:

- **Release**: The change of a chemical substance into a plant-accessible form, occurring through processes such as hydrolysis, degradation, or dissolution.
- **Slow-release**: The rate of nutrient release from fertilizer must be slower than the rate at which the nutrient can be readily absorbed by plants.
- **Declaration**: A fertilizer can be classified as slow-release if the nutrients declared as such meet each of the following three criteria, which are required to be met under specific conditions, such as a temperature of 25 °C:
  - No more than 15% of the nutrients are released within 24 hours.
  - No more than 75% of the nutrients are released within 28 days.
  - At least approximately 75% of the nutrients are released within the specified release time.

In general, the terms “slow-release fertilizers (SRFs)” and “controlled release fertilizers (CRFs)” can be used interchangeably and can be referred to as "Enhanced Efficiency Fertilizers (EEF)".

Slow-release fertilizers (SRFs) are commonly decomposed by microbes, resulting in the gradual release of nitrogen. Therefore, the SRFs nutrient release patterns are completely dependent on soil and climatic conditions. Natural SRFs include plant manure, cover crops, animal manures and compost. Synthetic SRFs are gradually dissolved in water. Urea-formaldehyde (UF), isobutylidene diurea (IBDU), and crotonylidene diurea (CDU) are examples of synthetic SRFs commonly used in agriculture.

Controlled-release fertilizers (CRFs) are usually coated or encapsulated with inorganic or organic materials. These coatings are responsible for regulating the rate, pattern, and duration of nutrient release to plants. The release rate of CRFs is carefully

designed to match the changing nutrient requirements of crops, improving nutrient use efficiency, reducing environmental impacts, and optimizing crop productivity.

The rate of nutrient release from SRFs can be influenced by various factors such as soil type, soil composition, and local climatic conditions. The slow-release fertilizers (SRF) mechanism is inherently unpredictable. In contrast, controlled release fertilizers (CRF) offer a predictable method, quantity, and rate of release in the soil [13].

2.3 Classification of slow-release fertilizers

The slow-release fertilizers (SRFs) can be widely categorized based on their composition, release mechanism, and type of coating as illustrated in the diagram in Figure 2.2. [14]

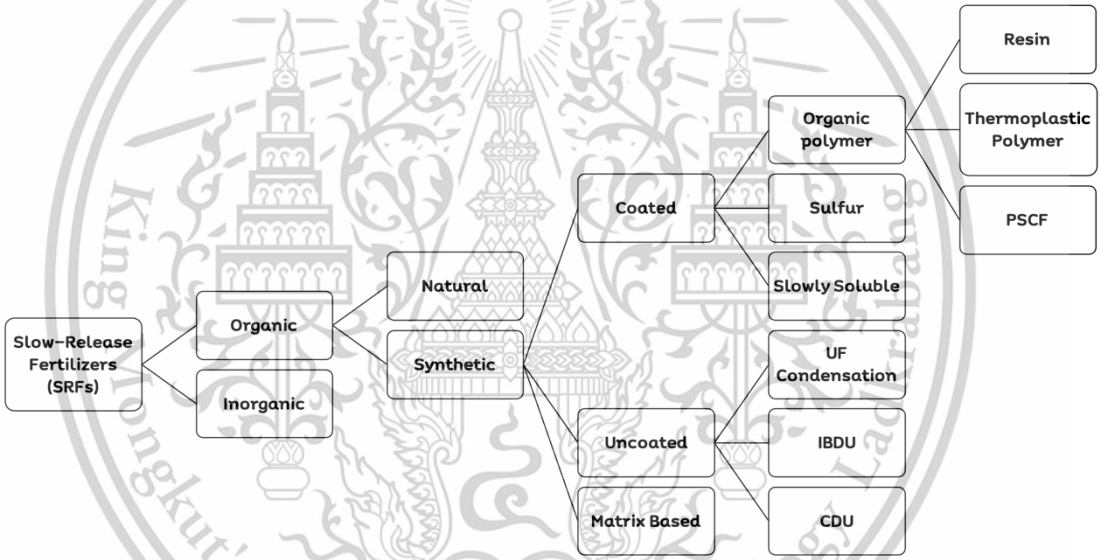

Figure 2.2 The classification of slow-release fertilizers (SRFs) [14].

2.3.1 Inorganic Low-solubility SRFs

This category comprises natural organic materials such as biomass, crops, animal products, animal manure, composts, activated sludge, and sewage sludge. Some of these products may contain beneficial bacteria. They exhibit slow to very slow nitrogen release and are relatively expensive in terms of cost per unit of nitrogen. However, they offer advantages such as low risk of burning and leaching. The release of nutrients from these fertilizers depends on soil temperature and biological activity, as they need warm soil conditions for conversion into ammonium and nitrate forms.

Many gardeners prefer natural organics due to their ability to improve soil quality. There are various types of natural organic fertilizers, each with unique characteristics. The release rates of nutrients vary greatly and are primarily influenced by soil bacteria and fungi, which are most active in warm soil temperatures. The higher the biological activity in the soil, the faster the nutrient release rate.

2.3.2 Organic SRFs

2.3.2.1 Natural Organic SRFs

This category comprises natural organic materials such as blood meal, wheat germ, soya, poultry manure, seed meals, cottonseed meal, soybean meal, fish emulsion, composts, activated sludge, and sewage sludge. Some of these products may contain beneficial bacteria. They exhibit slow to very slow nitrogen release and are relatively expensive in terms of cost per unit of nitrogen. However, they offer advantages such as low risk of burning and leaching. The release of nutrients from these fertilizers depends on soil temperature and biological activity, as they need warm soil conditions for conversion into ammonium and nitrate forms.

Many gardeners prefer natural organics due to their ability to improve soil quality. There are various types of natural organic fertilizers, each with unique characteristics. The release rates of nutrients vary greatly and are primarily influenced by soil bacteria and fungi, which are most active in warm soil temperatures. The higher the biological activity in the soil, the faster the nutrient release rate [15].

2.3.2.2 Synthetic Organic SRFs

2.3.2.2.1 Matrix-Based SRFs

These SRFs types are created by incorporating substances that reduce nutrient rate of dissolution, such as rubber, gel-based materials, and thermoplastic polymers. The rate at which these fertilizers dissolve depends primarily on the surface area relative to their volume. In other words, larger-sized SRFs release nutrients at a slower rate.

2.3.2.2.2 Uncoated SRFs

Uncoated SRFs exhibit a slow release because of the slow reaction. Non-coated materials with limited solubility are often produced in smaller particle sizes compared to coated products. One characteristic of uncoated products is their homogeneity, meaning that their composition remains consistent throughout the particle. Homogeneous fertilizers release nutrients at a rate that is not influenced by any coating. The examples of uncoated SRFs are as follows.

- **Urea-formaldehyde condensation (UF) – 38% N:** Urea and formaldehyde react at different levels, resulting in polymer chain molecules of varying lengths. Longer chains are formed as the reaction progresses, which in turn affects the release properties. UF reaction products undergo microbial degradation or hydrolysis in the soil solution, leading to the conversion of nitrogen (N) into a plant-available form. Microbial decomposition is the primary mechanism for nitrogen release. Factors such as soil temperature, moisture content, pH value, and oxygen availability affect the activity of microorganisms, which in turn impacts the rate of nitrogen release. Additionally, the length of the polymer chain in the UF material also plays a role in the rate of nitrogen release.
- **Isobutylidene diurea (IBDU®) – 32% N:** IBDU releases its nitrogen content through hydrolysis, wherein it reacts with water to form urea and isobutyraldehyde. The rate of hydrolysis is accelerated by low pH and high temperature, which is different from UF polymers that rely on soil bacteria for nitrogen release. In the case of IBDU, its solubility is primarily dependent on water. Its ability to dissolve in water controls the transportation of the product to the soil solution. The rate of dissolution is influenced by particle size and water availability. In the soil solution, hydrolysis occurs based on soil pH and temperature, with lower temperatures promoting faster hydrolysis. IBDU is particularly suitable for winter applications due to its moisture dependence [16].
- **Crotonylidene dirurea (CDU®) – 32.5% N:** Nitrogen is released from CDU through hydrolysis and microbial degradation in the soil. When CDU dissolves in water, it decomposes into urea and crotonaldehyde. Soil moisture and microbial activity affect the rate of nitrogen release. Particle size also plays a role, as larger particles tend to have slower release rates. Factors such as temperature, moisture, and pH levels in the soil can also impact the rate of nitrogen release. CDU is particularly effective in acidic soil conditions. The use of CDU is common in grass fields and specialized agriculture [17].

2.3.2.2.3 Coates SRFs

2.3.2.2.3.1 Organic polymer coated SRFs

- **Resin coated (Chelated Micronutrients) SRFs:** Resin-coated fertilizers are created through in-situ polymerization, resulting in the formation of a cross-linked, hydrophobic polymer. The two commonly used types of resins are alkyd-type resins (e.g., Osmocote) and polyurethane-like coatings (e.g., Polyon, Plantacote, and Multicote). The thickness of the coating determines the control over nutrient

release. Alkyd-type coatings offer better control over composition and thickness, allowing for precise regulation of the fertilizer's release rate and pattern. Polyurethane-like coatings involve reacting poly-isocyanates with polyols on the fertilizer granule's surface. This coating is unique because the poly-isocyanate reacts with the fertilizer core, creating durable SRFs that resists attrition. The release of nutrients from resin-coated fertilizers is primarily influenced by temperature, while factors such as soil moisture content, pH, wetting and drying cycles, and soil microbial activity have minimal effects on the release process [18].

- **Thermoplastic polymer-coated SRFs:** Thermoplastic polymer-coated slow-release fertilizers (PCFs) are highly efficient among slow-release fertilizers (SRFs) as they enhance product longevity and nutrient efficiency. PCFs utilize a diffusion-based nutrient release mechanism through a semi-permeable polymer membrane. They are coated with polymers such as low-permeability polyethylene or high-permeability ethylene-vinyl-acetate, with the release rate adjusted by varying the composition and thickness of the coating. The type of fertilizer substrate also affects the rate of nitrogen release.
  - *Meister products* utilize thermoplastic resins as coatings, which are applied to various substrates like urea, di-ammonium phosphate, potassium sulfate, potassium chloride, and ammonium nitrate. To control nutrient release, release-controlling agents such as ethylene-vinyl acetate and surfactants are added to the coating, while coating thicknesses generally remain consistent. Talc resin can also be blended into the coating to modify release rates. Nutrient release occurs through diffusion across the coating, and temperature plays a significant role in controlling the release rate.
  - *Reactive layer coating (RLC)* is a newer technology where two reactive monomers are simultaneously applied to the fertilizer substrate, creating an ultra-thin membrane coating. Nutrient release in RLC products is controlled by osmotic diffusion through this membrane. Various basic fertilizers, including urea, potassium nitrate, potassium sulfate, potassium chloride, ammonium sulfate, ammonium phosphate, and iron sulfate, are coated using RLC technology in different particle sizes. The coating thickness determines the diffusion rate and the duration of nutrient release.
  - *Multicote products* involve heating fertilizer granules in a rotating pan and applying layers of a fatty acid salt, followed by a paraffin topcoat. The coating weights for multicote products are relatively high compared to other

technologies, but this is offset by the lower cost of coating materials. Substrates used in multicote products include potassium nitrates, urea, and triple superphosphate.

- **Polymer coating of sulfur-coated fertilizers (PSCFs):** A product known as polymer-sulfur coated fertilizers (PSCFs) has been developed to provide controlled-release performance similar to polymer-coated fertilizers but at a lower cost. PSCFs utilize a primary sulfur coating, chosen for its affordability, along with a secondary polymer coat. The water permeability properties of the polymer control the diffusion of water into and out of the fertilizer particles. PSCFs demonstrate excellent resistance to abrasion and maintain their integrity during handling. As the outer coating is a hard polymer, there is no waxy residue left on application equipment. The diffusion rate is controlled by the composition and thickness of the polymeric film. Water enters the sulfur/polymer interface through capillary action and starts to dissolve the fertilizer core. The dissolved fertilizer is then released from the particle in a reverse sequence. This mechanism results in a more uniform release of nutrients compared to traditional sulfur-coated urea (SCU) fertilizers. Additionally, the combination coating reduces the impact of temperature on nutrient release, making it less temperature-sensitive than most polymer-coated fertilizers.

2.3.2.2.3.2 Sulfur-Coated SRFs (SCU)

Sulfur is chosen as the main coating material for sulfur-coated urea (SCU) due to its low cost and its value as a secondary nutrient. SCU particles consist of urea coated with a layer of sulfur, giving them a brown to tan or yellow appearance, depending on the source of urea. The nitrogen (N) content of SCUs can vary, typically ranging from 30 to 40%.

The release of nitrogen from SCU occurs when water penetrates micropores, cracks, or areas of incomplete sulfur coverage in the coating. This allows for the dissolution of urea within the core of the particle, resulting in a rapid release of nitrogen. In the case of wax-sealed SCUs, a dual-release mechanism is present. The wax sealant acts as a barrier that must be broken down by soil microbes to expose imperfections in the sulfur coating. This microbial activity is influenced by temperature, making the release properties of wax-sealed SCUs temperature-dependent. The rate of nitrogen release from a single SCU particle depends on the coating thickness and quality. It is important to note that excessively thick sulfur coating may hinder effective nitrogen release. In turf applications, SCUs can provide a

nitrogen supply for a period ranging from 6 to 16 weeks, depending on factors such as coating weight, nitrogen application rate, and environmental conditions.

2.3.2.2.3.3 Slow soluble-coated SRFs

These fertilizers possess low solubility characteristics. The most common type is MagAmp. It contains N-P-K in a 7-40-6 formulation. The fertilizer provides a controlled release of nutrients over a period of 3-4 months or 8-10 months, depending on the specific product. However, it is important to monitor iron, manganese, copper, and zinc levels as the high phosphate content can lead to their depletion. Additionally, ammonium toxicity may occur in low pH soils, so pH adjustments may be necessary when using MagAmp [19].

2.4 Advantages, disadvantages and environmental effects of slow-release fertilizers

2.4.1 Advantages

The use of slow-release fertilizers increases nitrogen utilization efficiency (NUE) and reduces nitrogen losses. When using controlled-release fertilizers, it is possible to reduce the recommended treatment rate by 20 to 30% while keeping the yield constant. In contrast to soluble conventional fertilizers, which can be toxic to seedlings and cause osmotic stress and specific damage to plants at different growth stages, slow-release fertilizers offer potential benefits in mitigating these risks. They can also help minimize ammonium ion damage and lodging. Additionally, slow-release fertilizers, especially those with a sigmoidal nutrient release pattern which ensures a consistent and balanced supply of nutrients to plants can reduce the risk of nutrient overload or deficiency. It therefore resulted in enhancing agronomic safety and suitable for co-situs applications.

Slow-release fertilizers offer the advantage of providing all the necessary nutrients for multiple crops or crops grown under plastic covers in a single application. This reduces the need for frequent fertilizer application and simplifies the fertilization process. By reducing the risk of toxicity and excessive salt content in substrates, slow-release fertilizers allow for the use of larger quantities of fertilizer, a practice known as "depot fertilization". This not only improves convenience but also leads to significant savings in labor, time, and energy. These benefits are highly valued by most users of slow-release fertilizers. [20].

2.4.2 Disadvantages

The drawbacks of slow-release fertilizers mainly arise from a lack of understanding regarding their optimal usage. One key challenge is the absence of a standardized approach for determining nutrient release patterns. This creates a disconnect between laboratory test results and the actual performance of nutrient release in the field. Excessive thickness of the coating can lead to a slow release of nutrients. On the other hand, some coated fertilizers may release certain elements too rapidly initially, resulting in potential crop damage. Moreover, some coatings may take a considerable amount of time to fully disintegrate, hindering their effectiveness.

Farmers typically prefer to adjust nitrogen fertilization to improve crops and productivity. However, the use of coated fertilizers can limit this flexibility, as once applied, the release of nutrients cannot be easily modified. Additionally, the cost of producing slow-release fertilizers remains higher compared to conventional mineral fertilizers. This cost factor contradicts the widespread adoption of slow-release fertilizers in agriculture [14].

2.4.3 Effects of slow-release fertilizers on the environment

Utilizing slow-release fertilizers that enhance nutrient usage efficiency (NUE), particularly for nitrogen, can significantly reduce the environmental impact of fertilizer application. These fertilizers promote better nutrient uptake by plants, resulting in less residual nutrients left in the soil that could potentially be lost to the environment. This improved nutrient utilization helps minimize environmental risks associated with fertilizer use.

Encapsulated slow-release fertilizers are specifically developed solutions to address various environmental and technical concerns in gardening, horticulture, and agriculture. Users who prefer coated fertilizers for their labor-saving benefits should also recognize the environmental advantages associated with the nitrogen release properties of these fertilizers.

A comprehensive evaluation should consider the following factors:

- The characteristics and mechanisms of nutrient release.
- The influence of environmental factors on nutrient uptake and release, such as temperature, moisture, aeration, bioactivity, root exudates, and soil type.
- The specific nutrient requirements of plants in different agricultural contexts.

2.5 Method of Analysis of Chemical Fertilizer [21]

2.5.1 Nitrogen (N)

2.5.1.1 Total Nitrogen (TN) (%)

The total nitrogen content analysis is performed using the **combustion method**, as specified in the "Notification of the Ministry of Agriculture and Cooperatives Re: Prescribing the Method of Analysis of Chemical Fertilizer B.E. 2559, Method 1.05.02."

The combustion method is employed to determine the total nitrogen content in a sample by burning it, which converts all nitrogen compounds into nitrogen gas. The amount of nitrogen gas produced is then measured and compared with nitrogen standards for accurate quantification.

Equipment/chemicals

- Combustion Instrument
- Sucrose
- Standard substance EDTA (Ethylene diamine tetra acetic acid)
- pure oxygen gas (99.7% or more)
- pure helium gas (99.999% or more)

Analytical methods

1. Nitrogen standard graph preparation:
   - Take at least six samples from different positions of the EDTA standard to ensure representative nitrogen content, then weigh the EDTA standard.
   - Add sucrose to the samples, using an amount that is at least 0.5 times the total weight of the working standards.
   - Put the standard materials in tin foil or crucible then burn it in a high-temperature furnace.
   - Measure the amount of total nitrogen to create a standard graph.
2. Sample analysis:
   - Weigh 0.05xx - 0.1xxx g of sample and add sucrose in an amount that is not less than 0.5 times of the total weight of sample.
   - Place the sample in tin foil or crucible and transfer it to the high-temperature furnace and record the total nitrogen concentration (%).

2.5.2 Phosphorus (P)

2.5.2.1 Total Phosphorus (TP_2O_5) (%)

An analysis of the total phosphorus content is conducted using the Spectrophotometric Molybdovanadophosphate Method, which is specified in the "Notification of the Ministry of Agriculture and Cooperatives Re: Prescribing the Method of Analysis of Chemical Fertilizer B.E. 2559, Method 1.09.01."

The Spectrophotometric molybdovanadophosphate method is an analytical technique used to determine the total phosphorus content in fertilizer samples. In this method, the sample is digested using a mixture of perchloric acid and nitric acid. This digestion process converts the phosphorus in the fertilizer sample into a phosphate solution. Then, a Molybdovanadate solution is added to initiate a color reaction, which can be measured. The intensity of the color is proportional to the phosphorus concentration in the sample, and it is compared to a Phosphorus standard solution to determine the phosphorus content accurately.

Equipment/chemicals

- Spectrophotometer
- Digestion block with tube
- Ammonium metavanadate (NH_4VO_3), AR grade
- Ammonium molybdate [$(NH_4)6Mo7O_{24}.4H_2O$], AR grade
- Nitric acid 69 – 70% (HNO_3), AR grade
- Perchloric acid 69 – 72% ($HClO_4$), AR grade
- Potassium dihydrogen phosphate (KH_2PO_4), AR grade

Analytical methods

1. Reagent preparation:
   - Mix HNO_3 and $HClO_4$ at a 1: 1 ratio.
   - Prepare the Molybdovanadate solution by combining Ammonium molybdate and Ammonium metavanadate in specific quantities with water and $HClO_4$.
2. Standard solution preparation:
   - Prepare a 1000 ppm Phosphorus standard solution using KH_2PO_4.
   - Prepare a 100 ppm Phosphorus standard solution by diluting the 1000 ppm solution.
   - Prepare working standards solution with concentrations of 1, 2, 4, 6, 8, 10, and 12 ppm by further diluting the 100 ppm solution.

3. Sample solution preparation:
   - Weigh a sample (0.2xxx – 1.xxxx g) and place it in Erlenmeyer flask or digestion tube.
   - Add the mixed acid (HNO_3 and $HClO_4$) to digest the sample.
   - Transfer the sample solution to a volumetric flask, adjust the volume with water, and filter if necessary.
4. Analytical method:
   - Pipet a suitable amount of the sample solution into a volumetric flask.
   - Add the Molybdovanadate solution and adjust the volume with distilled water and leave for 30 minutes.
   - Measure the absorbance (A) or transmittance (%T) of the solutions using a spectrophotometer at a wavelength of 420 nm.
   - Compare the analytical results of the sample solution with the analytical graph of standard solution to determine the phosphorus concentration.

<u>Calculation</u>

$$\%\ P = \frac{\text{ppm} \times \text{dilution factor}}{\text{wt.of sample (g)} \times 10^6} \times 100$$

$$\%\ P_2O_5 = \%\ P \times 2.2914$$

ppm = The concentration of the solution sample from the standard graph (ml/L).

$$2.2914 = \frac{\text{molecular weight of } P_2O_5}{2 \times \text{atomic weight of P}}$$

2.5.2.2 Citrate insoluble phosphorus (CIP_2O_5) (%)

The analytical method described in the "Notification of the Ministry of Agriculture and Cooperatives Re: Prescribing the Method of Analysis of Chemical Fertilizer B.E. 2559, Method 1.10.01" was employed to determine the insoluble phosphorus content in ammonium citrate solution and the soluble phosphorus content in water.

The spectrophotometric molybdovanadophosphate method was utilized. The sample is dissolved and induced color formation with a molybdovanadate solution. This method involves using a spectrophotometer to measure the absorption of light at a specific wavelength and determine the intensity of light that passes through the

sample. To analyze the phosphorus content, the sample was treated differently based on its solubility.

For insoluble phosphorus in ammonium citrate solution, the sample was extracted with pH 7 ammonium citrate solution at 65 °C for 1 h. The resulting precipitate was digested using a mixture of perchloric acid and nitric acid. The soluble phosphorus in the fertilizer samples was then measured by adding a molybdovanadate solution and analyzing the light intensity at 420 nm using a spectrophotometer, comparing it with a phosphorus standard solution.

For soluble phosphorus in water, the sample was dissolved in distilled water, and the resulting solution was also colored with a molybdovanadate solution. The phosphorus content was determined by measuring the light intensity at 420 nm using a spectrophotometer and comparing it with a phosphorus standard solution.

Equipment/chemicals

- pH meter
- Shaking water bath
- Spectrophotometer
- Ammonium hydroxide 28 - 29% NH_3 (NH_4OH), AR grade
- Ammonium metavanadate (NH_4VO_3), AR grade
- Ammonium molybdate [$(NH_4)_6Mo_7O_{24}.4H_2O$], AR grade
- Citric acid ($C_6H_8O_7.H_2O$), AR grade
- Nitric acid 69 - 70% (HNO_3), AR grade
- Perchloric acid 69 - 72% ($HClO_4$), AR grade
- Potassium dihydrogen phosphate (KH_2PO_4), AR grade

Analytical methods

1. Reagent preparation:
   - Mix HNO_3 and $HClO_4$ in a 1:1 ratio by volume.
   - Prepare the Molybdovanadate solution by combining Ammonium molybdate and Ammonium metavanadate with water and $HClO_4$.
   - Dilute Ammonium hydroxide with water in a 1:7 ratio by volume.
   - Prepare Ammonium citrate solution by dissolving citric acid in water and adjusting the pH to 7 using diluted Ammonium hydroxide and Citric acid.

2. Standard solution preparation:
   - Prepare a 1000 ppm Phosphorus standard solution using KH_2PO_4.
   - Prepare a 100 ppm Phosphorus standard solution by diluting the 1000 ppm solution.
   - Prepare working standards solution with concentrations of 1, 2, 4, 6, 8, 10, and 12 ppm by further diluting the 100 ppm solution.
3. Sample solution preparation:

3.1. For insoluble phosphorus in ammonium citrate solution:
   - Weigh sample (0.9xxx - 1.0xxx g) into a flask.
   - Add 100 ml ammonium citrate solution and put in shaking water bath at 65 °C for 1 hour.
   - Filter and transfer sediment with filter paper to a flask.
   - Add mixed acid (20 ml) and digest until clear.
   - Transfer to a volumetric flask (100 ml or 250 ml), adjust volume with water.

3.2. For soluble phosphorus in water:
   - Weigh 0.9xxx - 1.0xxx g of the sample into a 250 ml volumetric flask.
   - Add 100 ml of water, shake thoroughly for 30 min.
   - Adjust the volume with water and shake again.

4. Analytical methods:
   - Pipette sample solution into a flask (25 ml), then add Molybdovanadate solution, adjust volume with water, leave the sample for 30 min.
   - Take working standards (1-7 ppm), add Molybdovanadate solution (10 ml), adjust volume with water.
   - Measure the color intensity of solutions using a spectrophotometer at a wavelength of 420 nm, then record the absorbance (A) or transmittance (%T).
   - Determine sample concentration by comparing it with a standard graph.

Calculation

$$\% P = \frac{\text{ppm} \times \text{dilution factor}}{\text{wt.of sample (g)} \times 10^6} \times 100$$

$$\% P_2O_5 = \% P \times 2.2914$$

ppm = The concentration of the solution sample from the standard graph (ml/L).

$$2.2914 = \frac{\text{molecular weight of } P_2O_5}{2 \times \text{atomic weight of P}}$$

2.5.2.3 Available Phosphorus (AVP_2O_5) (%)

The analytical method described follows the guidelines outlined in "Notification of the Ministry of Agriculture and Cooperatives Re: Prescribing the Method of Analysis of Chemical Fertilizer B.E. 2016, Method 1.11.01." This method is used to determine the useful phosphorus content in fertilizer samples, reported as P_2O_5.

The method used for analyzing useful phosphorus involves an indirect method. The analysis involves subtracting the results of the total phosphorus analysis from the results obtained through the analysis of insoluble phosphorus in an ammonium citrate solution.

Equipment/chemicals

- Tools, materials, and equipment are according to methods 1.09.01 and 1.10.01.
- Chemicals are according to methods 1.09.01 and 1.10.01.

Analytical method

- Total Phosphorus Analysis (1.09.01)
- Citrate insoluble phosphorus (1.10.01)

Calculation

% Available P_2O_5 = Total P_2O_5 - Citrate insoluble P_2O_5

2.5.3 Potassium (K)

2.5.3.1 Water Soluble Potassium (WK_2O) (%)

The analytical method used is the **Inductive Couples Plasma Emission Spectroscopic method**, as described in "Notification of the Ministry of Agriculture and Cooperatives Re: Prescribing the Method of Analysis of Chemical Fertilizer B.E. 2559, Method 1.12.02". This method is employed to analyze the concentration of dissolved potassium in chemical fertilizers, reported as K_2O.

The concentration of dissolved potassium was measured using an Inductively Coupled Plasma Atomic Emission Spectrometer (ICP-OES/ICP-AES). In this method, the sample solution is heated by a high-energy plasma generated by argon gas. The energized substance undergoes ionization and emits light energy at various wavelengths. The intensity of light at a specific wavelength is then measured. The measured light intensity is directly proportional to the concentration of potassium in the solution.

Equipment/chemicals

- Inductively coupled plasma atomic emission spectrometer (ICP-OES/ICP-AES)
- Precision scales (4 decimal places)
- Potassium Standard Solution (K) 1000 ppm

Analytical method

1. Preparation of Potassium Standard Solution as Working standard:
   - Transfer 1000 ppm potassium standard solution to at least 6 different concentrations ranging from 0 to 300 ppm.
   - Pipette each concentration into a 100 ml volumetric flask and adjust the volume with distilled water and thoroughly mix the solutions by shaking.
2. Sample solution preparation:
   - Weigh a sample ranging from 0.25xx to 1.xxxx g into a 500 ml volumetric flask.
   - Add 200 ml of distilled water and shake thoroughly using a shaker for 1 h.
   - If there is any precipitation, filter the solution through filter paper No. 1.
3. Analytical method
   - Pipette an appropriate volume of the sample solution (from No. 2) into a 50 ml volumetric flask, adjust the volume with distilled water and shake thoroughly.
   - Use an inductively coupled plasma atomic emission spectrometer to measure the potassium content in both the working standard (from No. 1) and the sample solution (from No 3).
   - Determine the concentration of the sample solution by comparing the analytical results with a standard graph that illustrates the relationship between the potassium concentration and the emission intensity of the working standard.

Calculate

$$\% \text{ K} = \frac{\text{ppm} \times \text{dilution factor}}{\text{wt.of sample (g)} \times 10^6} \times 100$$

$$\% \text{ } K_2O = \% \text{ K} \times 1.2046$$

ppm = The concentration of the sample solution from the standard graph (ml/L).

$$1.2046 = \frac{\text{molecular weight of } K_2O}{2 \times \text{Atomic weight of K}}$$

2.6 The release rate of nutrients from fertilizer

Test methods for determining the release rate of nutrients from slow-release fertilizers can vary depending on the specific fertilizer type and release mechanism. One commonly employed method is the static soaking method. In this approach, the slow-release fertilizer is immersed in water or solution for a defined period. Samples of the solution are collected at regular intervals, and the concentration of nutrients is analyzed using techniques such as spectrophotometry, inductively coupled plasma (ICP), or ion-selective electrodes.

During the static soaking test, the slow-release fertilizer is allowed to release nutrients into the surrounding solution. The samples taken at different time points enable monitoring of the nutrient release kinetics. Analytical techniques like spectrophotometry can measure the concentration of specific nutrients, while ICP allows for the simultaneous determination of multiple elements. Ion-selective electrodes are useful for detecting specific ions in the solution.

2.6.1 Example Research: Release Characteristics of Nutrients from Polymer-coated Compound Controlled Release Fertilizers [22]

This study conducted an experiment to investigate the release rates of different nutrients (nitrate, ammonium, phosphate, and potassium) from a polymer-coated fertilizer (F1=19:6:13 and F2=18:6:12). The experiment involved immersing 5 grams of coated fertilizer in 33.3 ml of DI water at different temperatures (20°C, 30°C, and 40°C), with four replicates for each treatment.

During the experiment, the supernatant solutions (the liquid above the settled solids) were collected at specific time intervals. Initially, samples were taken every two days for the first 20 days, and then the intervals were increased to every five days. After each sampling, the water was replaced with fresh DI water.

The concentrations of nutrients in the collected samples were analyzed using a Lachat auto-analyzer for nitrate, ammonium, and phosphate, and an Optima 1000 ICP instrument for potassium. The release rates of the nutrients were compared over time.

Figure 2.3 shows the release behavior of potassium, nitrate, ammonium, and phosphate from CRF-F1 and CRF-F2 at 20°C and 40°C. The release rates of CRFs samples are shown in Table 2.2. The study revealed variations in the release rates among different nutrients from polymer-coated fertilizers. Nitrate had the fastest

release rate, followed by ammonium and potassium, while phosphate had a significantly slower release rate. The findings emphasize the importance of considering nutrient release dynamics and selecting appropriate fertilizer formulations based on specific plant requirements and soil characteristics.

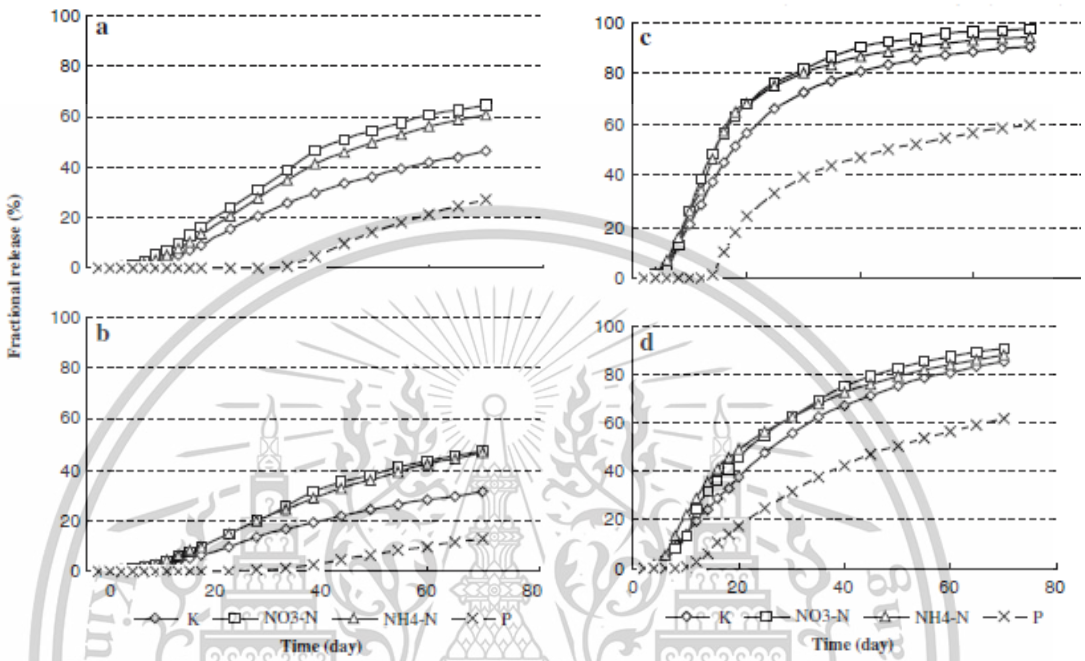

Figure 2.3 Release of potassium, nitrate, ammonium, and phosphate from (a) CRF-F1 at 20°C, (b) CRF-F2 at 20°C, (c) CRF-F1 at 40°C, and (d) CRF-F2 at 40°C [22].

Table 2.2 Release rates (%per day) of nitrate, ammonium, potassium, and phosphate during the linear period for CRF-F1 and CRF-F2 in free water at different temperatures.

Nutrients	$CRF\text{-}F_1$			$CRF\text{-}F_2$		
	20 °C	30 °C	40 °C	20 °C	30 °C	40 °C
NO_3-N	1.04 ± 0.02	2.04 ± 0.04	3.32 ± 0.06	0.76 ± 0.02	1.35 ± 0.02	2.24 ± 0.04
NH_4-N	0.98 ± 0.02	1.85 ± 0.03	3.26 ± 0.02	0.75 ± 0.02	1.49 ± 0.02	2.24 ± 0.05
K	0.75 ± 0.02	1.43 ± 0.04	2.59 ± 0.05	0.51 ± 0.01	0.93 ± 0.03	1.56 ± 0.04
P	0.77 ± 0.02	0.89 ± 0.03	2.1 ± 0.02	0.32 ± 0.01	0.65 ± 0.01	1.03 ± 0.02

2.6.2 Example Research: Slow-release NPK fertilizer encapsulated by carboxymethyl cellulose-based nanocomposite with the function of water retention in soil [23]

This study attempted to prepare a novel SRF formulation based on SCMC-g-poly(AA)/PVP/Silica (Hyd/PVP/Silica). To investigate the release of NPK fertilizer from a synthesized slow-release fertilizer (SRF), the experiment involved placing 0.05 g of the SRF formulation inside a dialysis bag, which was then immersed in 100 mL of distilled water. At specific time intervals, a 10 mL sample of the solution was collected for NPK fertilizer analysis. To maintain a constant volume, 10 mL of additional distilled water was added to the beaker. The amount of fertilizer released from the SRF formulation was determined using a digital conductivity meter and a calibration curve. The fertilizer concentration was calculated based on a standard curve, and the cumulative release was calculated using the following equation.

$$\mathrm{E} = \frac{V_E \sum_1^{n-1} C_i + V_0 C_n}{m_0} \times 100 \qquad (2.1)$$

Where

E is the accumulative release (%) of NPK fertilizer,

$\mathbf{V_E}$ and $\mathbf{V_0}$ are the sampling volume and the initial volume of release medium (mL),

$\mathbf{C_i}$ and $\mathbf{C_n}$ are the fertilizer concentrations (mg/mL), **i** and **n** are the sampling times, and $\mathbf{m_0}$ is the mass of fertilizer in the SRF formulation (mg).

The fertilizer release profile of different formulations, namely pure NPK, Hyd/NPK, Hyd/PVP/NPK, and Hyd/PVP/silica/NPK, was studied using conductivity measurements over time in water, as shown in Figure 2.4. Pure NPK fertilizer exhibited rapid dissolution in water, with complete release achieved within 6 h. On the other hand, the formulations containing hydrogel matrices, such as Hyd/NPK, Hyd/PVP/NPK, and Hyd/PVP/silica/NPK, demonstrated sustained release behavior due to the barrier effect of the polymeric matrix within the hydrogel network. Within the specified time periods, the release of fertilizer content in each formulation can be summarized as follows:

Within 1 day:

- Hyd/NPK released 31% of the fertilizer content.
- Hyd/PVP/NPK released 16.9% of the fertilizer content.
- Hyd/PVP/silica/NPK released 11.2% of the fertilizer content.

Within 1 week:

- Hyd/NPK released 62.1% of the fertilizer content.
- Hyd/PVP/NPK released 44.5% of the fertilizer content.
- Hyd/PVP/silica/NPK released 32.1% of the fertilizer content.

Within 1 month:

- Hyd/NPK released 89% of the fertilizer content.
- Hyd/PVP/NPK released 75.3% of the fertilizer content.
- Hyd/PVP/silica/NPK released 65.3% of the fertilizer content.

The Hyd/PVP/silica/NPK formulation exhibited excellent slow-release properties for fertilizer release in distilled water. The cumulative release within the first day was below 15%, and over one month, it remained below 75%. These results indicate a controlled and prolonged nutrient release, meeting the standards set by the Committee of European Normalization (CEN) for slow-release fertilizers.

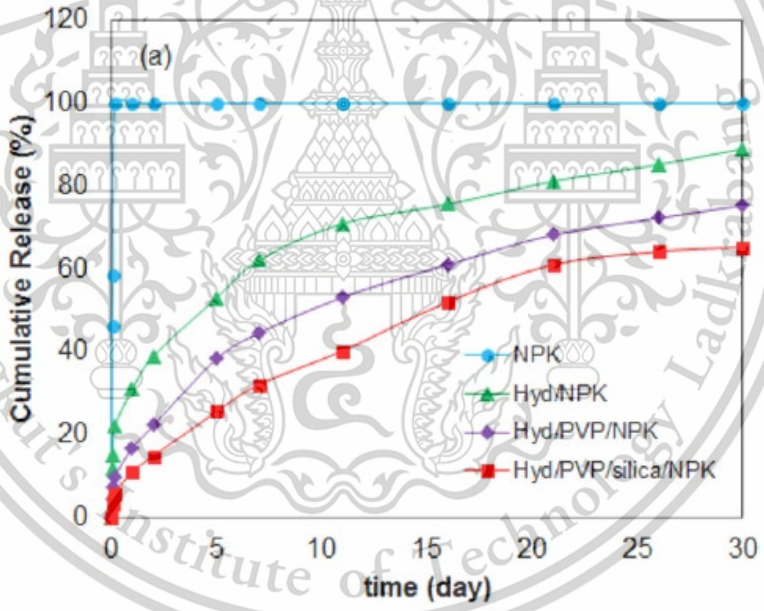

Figure 2.3 Release behaviors of four types of fertilizer formulations in distilled water.

2.7 Literature reviews

Olad et al. (2018) [23] investigated the synthesis of a slow-release fertilizer by encapsulating NPK fertilizer within a superabsorbent nanocomposite. The encapsulation process involved polymerizing sulfonated-carboxymethyl cellulose (SCMC) with acrylic acid (AA) in the presence of polyvinylpyrrolidone (PVP) and silica. The resulting hydrogel nanocomposites demonstrated excellent slow-release properties for the fertilizer. The release behavior of the fertilizer from the encapsulated hydrogel was found to be in accordance with the standards of Committee of European Normalization (CEN). The encapsulation technique offers the potential for controlled nutrient release, which can enhance nutrient utilization efficiency and reduce environmental impact.

Rashidzadeh et al. (2014) [24] prepared a novel slow-release NPK fertilizer by encapsulating it within a superabsorbent nanocomposite. The encapsulation process involved in-situ free radical polymerization of sodium alginate, acrylic acid, acrylamide, and montmorillonite in the presence of fertilizer compounds. The presence of montmorillonite contributed to a more controlled release of fertilizer in the system. The new fertilizer slow release in distilled water and soil indicated that the fertilizer release properties of superabsorbent nanocomposite with MMT conformed to the standard of slow-release fertilizers. The findings of this study highlight the potential of using superabsorbent nanocomposites containing montmorillonite for the development of slow-release fertilizers.

Rob et al. (2018) [25] developed a slow-release fertilizer (SRF) composite by incorporating nano-hydroxyapatite (nano-HA) and water-soluble fertilizers (urea, $(NH_4)_2HPO_4$, and K_2SO_4) into a hydrogel made from water hyacinth cellulose-graft-poly(acrylamide) polymer. The SRF exhibited a gradual increase in mineral nitrogen (MN) content between the 8th and 12th week, followed by a decline in the 16th week. This indicates a sustained release of nitrogen over an extended period. In comparison, conventional fertilizer (CF) released a higher amount of MN in the initial weeks but did not maintain consistent nutrient availability. Available phosphorus (P) content showed variability among treatments, with certain SRFs releasing higher P content than CF in the 8th week. This demonstrates the ability of the SRF composite to regulate phosphorus release. Exchangeable potassium (K) showed minimal variation, suggesting a short release time for this nutrient. The study highlights the potential of the SRF composite to enhance nutrient availability and utilization in agricultural systems by providing a controlled and sustained nutrient release.

Zhang et al. (2020) [26] prepared a hydrogel slow-release nitrogen fertilizer utilizing sawdust as a base material through grafting copolymerization. The fertilizer incorporated urea as the nitrogen source within the hydrogel structure. Potassium persulfate (KPS) and N,N'-methylenebis acrylamide (MBA) were employed as the initiator and crosslinker, respectively. The nitrogen release from the fertilizer exhibited an initial slow-release rate, which gradually increased over time. Then, the nutrient release rate reached a gentle and sustained pattern. This behavior can be attributed to the gel strength of the hydrogel network. As gel strength decreased, the nutrient release rate gradually increased, indicating the influence of the hydrogel structural on nutrient release kinetics.

Ramli et al. (2019) [27] developed a slow-release fertilizer hydrogel (SRFH) known as Coco peat-grafted-poly(acrylic acid)/NPK [CP-g-P(AAc)/NPK] by grafting coco peat fiber onto acrylic acid in the presence of NPK 15-15-15 fertilizer through in-situ solution polymerization. The properties of the SRFH were compared to those of a commercial super absorbent polymer (CSAP). Differential scanning calorimetry (DSC) analysis revealed that the SRFH exhibited a higher glass transition temperature (Tg) compared to CSAP. Scanning electron microscopy (SEM) images showed that the SRFH had a more compact and less porous structure compared to the CSAP. Fertilizer release studies demonstrated that the SRFH exhibited improved nutrient release, indicating its potential as an efficient slow-release fertilizer.

Gumelar et al. (2020) [28] developed slow-release fertilizer (SRF) technology that involves the application of a chitosan coating on the surface of fertilizer granules. The coating process is carried out using liquid chitosan, which is sprayed onto the granules in a rotary pan granulator. The chitosan coating provides resistance to water, allowing for a controlled release of nutrients over a period of 3-6 months. In the case of SRF NPK16-16-16 coated with chitosan, the release of nutrients was evaluated. Within a month of immersion time, the coated fertilizer released approximately 103.26 mg of nitrogen (N), 21.8 mg of phosphorus (P), and 65.62 mg of potassium (K). These nutrient release amounts were lower compared to uncoated fertilizer over a 4-week period. The presence of chitosan particles in the NPK fertilizer resulted in a slower release rate of N, P, and K nutrients. This indicates that the application of chitosan particles enhances fertilizer efficiency by reducing nutrient leaching and providing a more controlled release of nutrients.

Pang et al. (2018) [29] fabricated a novel slow-release fertilizer (SRF) using lignin-based microcapsules. The microcapsules were prepared by coating K_2HPO_4 and

urea with lignin and formaldehyde, resulting in an NPK compound SRF. The release of nitrogen (N), phosphorus (P), and potassium (K) from the SRF was evaluated in water and soil environments. After 5 days, the release amounts of N, P, and K in water were 95.39%, 95.28%, and 96.75%, respectively. In soil, the release amounts were 83.35% for N, 96.62% for P, and 90.75% for K. The release of NPK from the SRF was influenced by environmental factors. Higher temperatures and acidic conditions promoted the release, while alkaline environments inhibited it. The results demonstrated that the lignin-based microcapsules exhibited good slow-release properties, making them suitable for efficient nutrient delivery in agricultural production.

Ghumman et al. (2022) [30] reported the preparation of novel slow-release fertilizer enriched with sulfur and urea. It was developed using a sustainable hydrophobic and biodegradable crosslinked copolymer Poly(S-RSO), which was synthesized from sulfur and rubber seed oil. The dip coating method was employed to coat the fertilizers with Poly(S-RSO). In a nitrogen release test conducted in distilled water, it was observed that the coated fertilizers with different coating thicknesses (165 µm, 254 µm, and 264 µm) released only 65% of their total nutrient content after 2, 19, and 43 days of incubation, respectively. This demonstrated excellent slow-release properties. In soil, the fertilizer with a coating thickness of 264 µm released only 17% of its nitrogen content after 20 days of incubation, meeting the standards set by the European standard (EN 13266, 2001). The newly developed slow-release fertilizers exhibited outstanding slow-release characteristics and improved sulfur oxidation when compared to existing coated fertilizers.

Boutriouia et al. (2022) [31] fabricate a coating material with controlled and slow-release properties for water-soluble fertilizer. A process was undertaken where polymethyl methacrylate (PMMA) was grafted onto carboxymethyl cellulose (CMC) through in-situ polymerization. Potassium persulfate (KPS) was used as the initiator for the polymerization reaction. Subsequently, the prepared copolymers were employed to coat conventional water-soluble diammonium phosphate (DAP) fertilizer in a laboratory rotary drum. The successful coating of the nanomaterials exhibited a significant delay in the release rate of nitrogen (N) and phosphorus (P) both in water and soil, compared to the release rate observed with uncoated fertilizers. This indicates that the coated fertilizers effectively controlled the release of N and P, leading to a slow-release effect. Furthermore, the coating agent demonstrated aerobic biodegradation, highlighting its environmental compatibility.

Chapter 3

Research methodology

The research methodology consists of two main parts. The first part focuses on investigating the formation conditions of LWAs. This includes studying the optimal mixing ratio of clay, expanded perlite (EP), and binder, as well as determining the sintering temperature within the range of 800–1000°C. The objective is to identify the conditions that yield LWAs with desired characteristics such as appropriate bulk density, porosity, and water absorption. In the second part, the research explores the incorporation of fertilizers into clay balls. This involves examining suitable absorbing media and determining the method for incorporating the fertilizers into the clay balls effectively. Figure 3.1 shows the schematic representation of the experimental procedure for the fabrication, characterization, fertilizer incorporation, and nutrient release evaluation of EP-LWA pellets. The process includes raw material preparation, palletization, sintering, physical property assessment, fertilizer loading using NPK solution, microstructural and elemental analysis, and nutrient release testing, followed by comparative analysis with commercial LWAs.

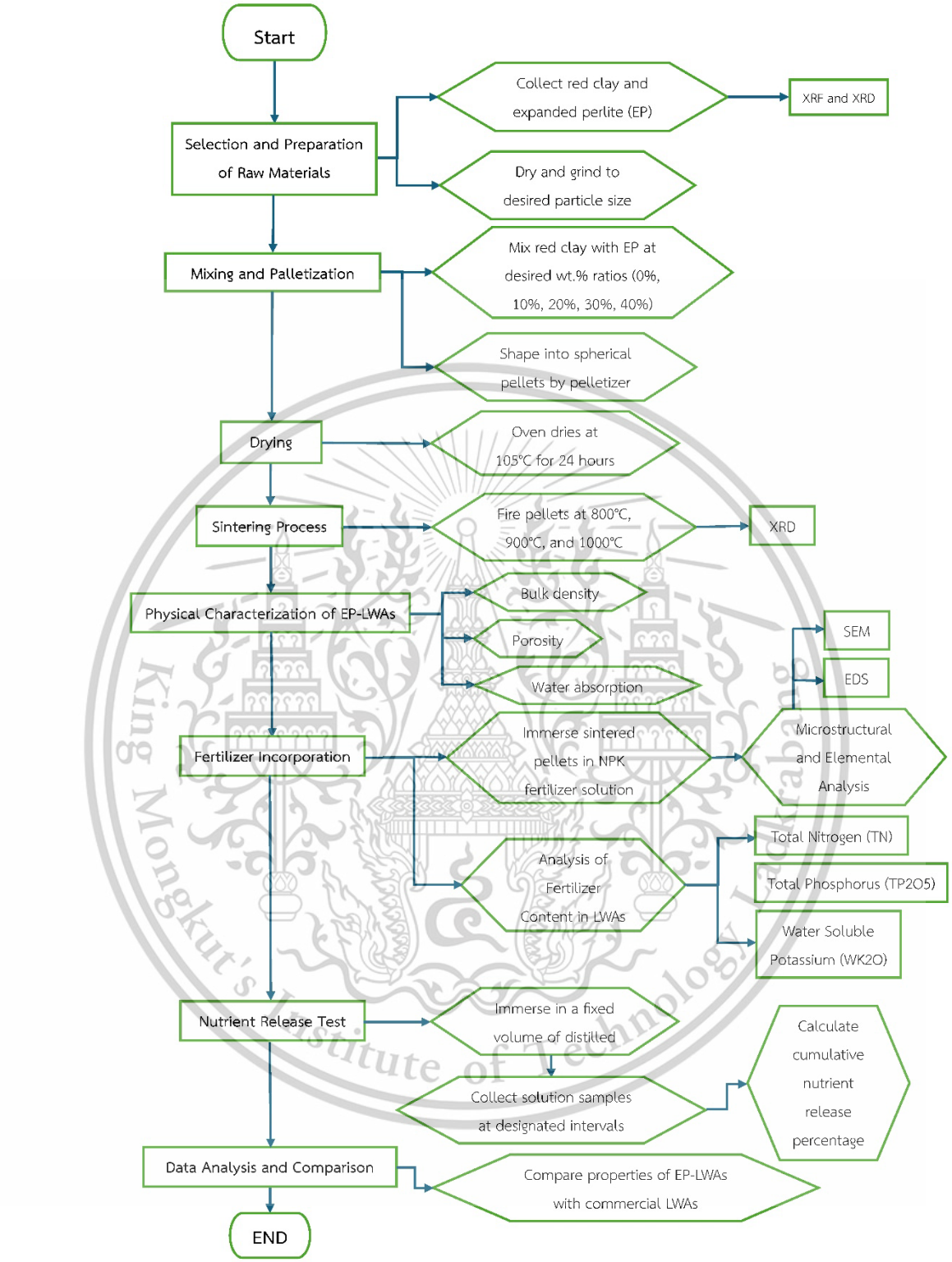

Figure 3.1. Schematic representation of the experimental procedure for the fabrication and characterization EP-LWA pellets.

3.1 Raw Materials and Experimental Equipment

3.1.1 Raw materials

(Figure 3.1)

1) Raw red clay from Phan Thong District, Chonburi Province
2) Expanded perlite (EP) from Klongyang Co., Ltd.
3) Carboxymethyl cellulose (CMC) from Chemipan Corporation Co., Ltd.
4) Compound fertilizer formula 16-16-16 from Chai Tai

(a) (b) (c) (d)

Figure 3.2. Raw Materials (a) Raw red clay, (b) Expanded perlite (EP), (c) CMC and (d) Fertilizer 16-16-16.

3.1.2 Equipment

(Some of equipments are shown in Figure 3.2)

1) Mixing vessels and stainless-steel trays.
2) Beaker
3) Precision balance 2 digits (Ohaus brand)
4) Analytical Balance 4 Digits and Archimedes density measuring device (Ohaus brand, model PX224 Pioneer)
5) Alumina crucible
6) Oven (Memmert brand, model UN55)
7) Electric kiln (Fisher Scientific brand, model 550-126)
8) Digital Hotplate and Stirrer for the preparation of specimens for the Archimedes density test.
9) Digital vernier caliper (Mitutoyo brand, model 500-196-30)
10) Mortar and pestle

11) Vacuum pump (VALUE VRI-4, Value Vacuum Technology, China; ultimate pressure 2 × 10^{-1} Pa, flow rate 4.0 m^3/h)

12) Erlenmeyer flask

Figure 3.3. Equipment (a) Precision balance 2 digits, (b) Analytical balance 4 digits, (c) Digital hotplate and stirrer, (d) Vacuum pump, (e) Alumina crucible, (f) Electric kiln, (g) Oven, and (h) Digital vernier caliper.

3.2 Fabrication processes

3.2.1 Preparation of LWAs

The preparation of LWAs involves a series of steps, as illustrated in Figure 3.3.

1) Red clay and expanded perlite (EP) were pulverized and sieved through a 200-mesh (74 μm) sieve to achieve a uniform particle size distribution.
2) Dry-mix the sieved red clay and EP at the desired EP replacement ratio (0–40 wt.% EP) for 5 min. The mixing ratio is shown in Table 3.1.
3) Gradually add the 0.05 wt.% CMC solution and continue mixing for an additional 10 minutes.
4) Transfer the plasticized blend to a pelletizing machine and form spherical pellets of ~8 mm diameter.
5) The pellets were dried in an oven at 105℃ for 24 h to remove moisture content.
6) The dried pellets were placed in alumina crucibles and sintered in an electric furnace at temperatures of 800℃, 900℃, and 1000℃ for 2 h.

Figure 3.4. The process of preparing LWAs.

Table 3.1 The mixing ratio between the clay with the perlite.

Samples	Clay: Perlite (in %wt ratio)	Clay (g)	Perlite (g)
P0	100:0	500	0
P1	90:10	450	50
P2	80:20	400	100
P3	70:30	350	150
P4	60:40	300	200

3.2.2 Archimedes method to analyze physical properties of LWAs

After sintering, the physical properties of the porous ceramic pellets—namely bulk density, porosity, and water absorption—were evaluated in accordance with ASTM C20 [32]. The measurement steps are shown in Figure 3.4.

1) Put the pellets in DI water and boil them for 6 h to remove air from the pellets, leave it cool down at least 12 h.
2) Weigh the pellets in DI water to obtain **suspended weight (S)** and weigh them in air to obtain **saturated weight (W).**
3) Dry the pellets in an oven at 120 for 24 h. After cooking, weigh the pellets to obtain **dry weight (D).**
4) Calculate the **volume (V)** of the pellets by subtracting the suspended weight (S) from the saturated weight (W), V=**W-S.**
5) Use the obtained measurements to calculate the bulk density, porosity, and water absorption of the LWAs according to the following equation.

$$\text{Bulk Density} = \frac{D}{V} \tag{3.2}$$

$$\text{Porosity} = \frac{W - D}{V} \times 100 \tag{3.3}$$

$$\text{Water absorption} = \frac{W - D}{D} \times 100 \tag{3.4}$$

Figure 3.5. Archimedes method to analyze physical properties of fired-clay balls.

3.3 Incorporating the fertilizers into the LWAs: The process steps are shown in Figure 3.5.

1) Grind a compound fertilizer, NPK 16-16-16 (Chai Tai, Thailand) using a mortar and pestle until they become powder. Use 30 g, 40 g and 50 g of fertilizer for this process.
2) Dissolve the fertilizer powder in 100 mL of a 0.15 wt.% carboxymethyl cellulose (CMC) solution—chosen for its superior ability to absorb and retain fertilizer
3) The blend was agitated on a magnetic stirrer for 30 min to achieve complete homogenization, yielding the final NPK/CMC solution.
4) About 30 sintered EP-LWA pellets (weighing roughly 10 g in total) were submerged in the NPK/CMC solution and placed inside a ~9 L vacuum desiccator hooked to a two-stage rotary-vane vacuum pump (VALUE VRI-4; ultimate vacuum 2×10^{-1} Pa, 4.0 m^3/h), then evacuated to –760 mmHg (≈1.3 kPa).
5) Maintain the vacuum for 3 h, allowing the fertilizer solution to penetrate the LWAs through suction. This vacuum process facilitates the replacement of air within the pore of the LWAs with the solution, allowing the fertilizer to effectively penetrate the pellets.

6) After 3 h, remove the LWAs from the vacuum chamber and place them in an oven at a temperature of 70°C for 24 h.
7) The samples were formally labeled EP-LWA-F30, EP-LWA-F40, and EP-LWA-F50, denoting fertilizer loadings of 30 wt.%, 40 wt.%, and 50 wt.%, respectively.
8) Absorbing media such as glycerol and vegetable oil were also examined for comparative analysis.

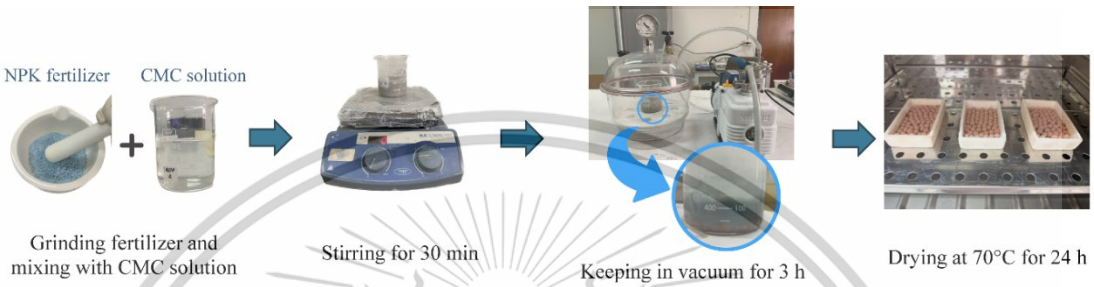

Figure 3.6. Diagram illustrating the sequential steps involved in introducing fertilizer into LWAs.

3.4 Analysis of chemical composition and microstructure of the starting material and LWAs

1) Analysis of the Elemental Composition of the Starting Material using X-ray Fluorescence (XRF) (Bruker S8 Tiger)

Experimental Procedure:

1. The raw material samples (e.g., red clay and expanded perlite) were first ground into fine powder using a mortar and pestle until the particle size passed through a 150-micron sieve (100 mesh) to ensure uniformity.
2. The powdered samples were then mixed with a binder (such as cellulose powder) in a suitable ratio to prepare pellets for analysis.
3. The mixture was pressed into pellets using a hydraulic press at a pressure of approximately 15–20 tons to form compact and stable pellets suitable for XRF measurement.
4. The prepared pellets were placed on the sample holder of the Bruker S8 Tiger XRF spectrometer.
5. Measurement parameters were set on the instrument, including the X-ray source (e.g., Rhodium target) and energy range, to cover the target elements. Each sample was analyzed for 60 to 120 seconds to obtain reliable signal intensity.

6. The XRF spectrometer detected the characteristic secondary X-rays emitted from the sample, which were used to determine the elemental composition.
7. The collected data were processed using the Bruker S8 Tiger software to quantify the major oxides and elements in the samples, reported as weight percentages (wt.%).
8. The results were verified for consistency by comparing with reference standards and previously reported data.

2) Analysis of the Crystalline Structure of the Starting Material and LWAs using X-ray Diffraction (XRD) (Rigaku Miniflex 800).

Experimental Procedure:

1. The powdered samples of raw materials and sintered lightweight aggregates were prepared by grinding them into fine powders passing through a 150-micron sieve to ensure homogeneity.
2. The powdered samples were carefully loaded onto a sample holder to form a flat, even surface for XRD measurement.
3. The sample holder was placed inside the Rigaku Miniflex 800 X-ray diffractometer.
4. The instrument was operated under the following conditions: Cu Kα radiation with a wavelength of 1.5406 Å, operating voltage of 40 kV, and current of 40 mA.
5. The diffraction patterns were recorded over a 2θ range of 5° to 70° with a step size of 0.02° and a scan speed of 2° per minute.
6. Each sample was scanned to obtain clear diffraction peaks, which represent the crystalline phases present in the material.
7. The obtained XRD patterns were analyzed and compared with standard reference patterns from the International Centre for Diffraction Data (ICDD) database to identify the crystalline phases.
8. Changes in peak positions and intensities were used to evaluate phase transformations after sintering at different temperatures.
9. The data were processed using Rigaku's software to generate graphs and phase identification reports for further interpretation.

3) Characterize the microstructure of the NPK- incorporated LWAs using field-emission scanning electron microscope (FEI Quanta 250, USA) equipped with an Oxford Instruments energy-dispersive X-ray (EDS) detector

Experimental Procedure:

1. Prepare small samples of the NPK-incorporated lightweight aggregates (LWAs) by cutting or crushing them into suitable sizes for microscopy analysis.
2. Mount the samples on aluminum stubs using conductive carbon tape to ensure good electrical contact.
3. Coat the samples with a thin layer of gold using a sputter coater to improve surface conductivity and image quality.
4. Place the prepared samples into the chamber of the FEI Quanta 250 field-emission scanning electron microscope.
5. Operate the microscope under high vacuum conditions to obtain clear microstructural images at various magnifications.
6. Use the Oxford Instruments energy-dispersive X-ray (EDS) detector attached to the FE-SEM to analyze the elemental composition at selected areas on the sample surface.
7. Collect and record high-resolution images and elemental maps to characterize the morphology and distribution of NPK fertilizer within the LWAs.

3.5 Analysis of chemical fertilizer in LWAs

The contents of fertilizer in clay ball are analyzed according to “Notification of the Ministry of Agriculture and Cooperatives Re: Prescribing the Method of Analysis of Chemical Fertilizer B.E. 2559” [33] as previously described in topic 2.5. The test method and standard number for each fertilizer are as follows.

- Total Nitrogen (TN): Combustion method (Method 1.05.02)
- Total Phosphorus (TP_2O_5): Spectrophotometric Molybdovanadophosphate Method (Method 1.09.01)
- Water Soluble Potassium (WK_2O): Inductive Couples Plasma Emission Spectroscopic method (Method 1.12.01)

Chapter 4

Results and discussion

This chapter presents the experimental results and ensuing discussion in three main sections—first, the chemical composition and phase analysis of the raw materials; second, the physical properties of the lightweight aggregates (LWAs) after sintering; and third, the analysis of fertilizer in NPK- incorporated LWAs.

4.1 Chemical composition and phase analysis of raw materials

The chemical compositions of red clay and expanded perlite were analyzed using X-ray fluorescence (XRF), with results shown in Table 4.1 Red clay is mainly composed of SiO_2 (66.9%), Al_2O_3 (22.3%), and Fe_2O_3 (4.85%), which contribute to its refractory nature and structural stability—especially important during sintering for improving thermal resistance and densification.

Expanded perlite, a volcanic glass, has a higher SiO_2 content (75.4%) but lower Al_2O_3 (13.6%) and Fe_2O_3 (1.33%). Its high silica enables strong thermal expansion and bloating, making it ideal for lightweight aggregate (LWA) applications. The presence of Na_2O (1.59%) and K_2O (6.75%) also aids sintering by acting as fluxing agents that support pore formation.

Table 4.1. The oxide chemical compositions of red clay and expanded perlite.

Component (wt%)	SiO_2	Al_2O_3	Fe_2O_3	K_2O	TiO_2	MgO	Na_2O	Na_2O	CaO	P_2O_5
Red clay	66.9	22.3	4.85	1.92	1.01	0.60	0.30	0.30	0.21	0.06
Expanded perlite	75.4	13.6	1.33	6.75	0.29	0.20	1.59	1.59	0.69	0.01

The phase compositions of raw materials identified by XRD are illustrated in Fig. 4.1. For the red clay sample (Fig. 4.1a), quartz (SiO_2) appears as the predominant crystalline phase, as indicated by the intense diffraction peak at 26.6°, corroborating XRF results that revealed a high SiO_2 content. Kaolinite ($Al_2Si_2O_5(OH)_4$) and illite ($KAl_2(Si_3Al)O_{10}(OH)_2$) are also present as the principal clay minerals, contributing to the plasticity and cohesion of the material. Hematite (Fe_2O_3) is confirmed by diffraction

peaks within the 33–35° range, which explains the characteristic red coloration of the clay due to iron oxides. Additionally, orthoclase feldspar ($KAlSi_2O_8$), identified by peaks around 27–29°, may function as a flux during sintering. The coexistence of these phases—quartz, kaolinite, illite, hematite, and feldspar—suggests that the red clay possesses favorable characteristics for lightweight aggregate (LWAs) production.

The XRD pattern of expanded perlite (Fig. 4.1b) is characterized by a broad halo between 15° and 35°, indicative of a predominantly amorphous silicate matrix, which is attributed to the rapid quenching of volcanic glass. Minor crystalline phases, likely including quartz and orthoclase, are evidenced by weak diffraction peaks. These structural features support the application of expanded perlite in enhancing the porosity of LWA materials.

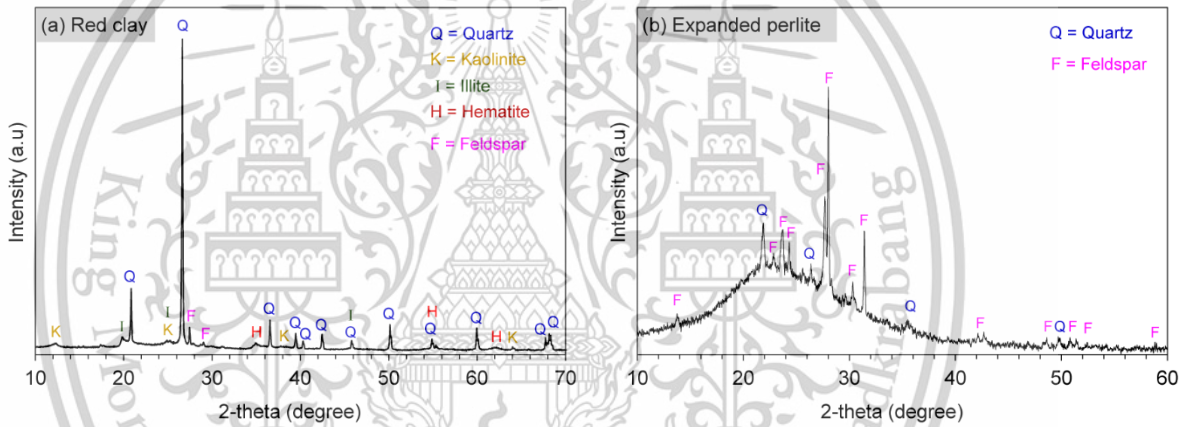

Figure 4.1. XRD patterns of phases identification in the raw materials: (a) red clay and (b) expanded perlite.

4.2 Physical properties of LWAs after sintering

Figure 4.2 presents the visual evolution in coloration of EP-LWAs containing (20 wt.% EP), both prior to and following sintering at various temperatures. Initially, the unfired clay pellets display a dark brown appearance, which gradually shifts to a pale orange hue when subjected to 800°C, with the color intensity increasing in correlation with rising sintering temperatures. Upon reaching 1000°C, the pellets exhibit a more intense reddish-orange coloration, indicating internal phase transformations. This chromatic shift is predominantly attributed to the presence of iron (Fe) in the raw clay, which undergoes oxidation during the sintering process. The emergence of hematite

(Fe_2O_3) a prevalent iron oxide responsible for the red and orange shades in fired ceramic materials—is central to this transformation. As temperature elevates, the oxidation of divalent iron (Fe^{2+}) to trivalent iron (Fe^{3+}) becomes more extensive, thereby enhancing the reddish-orange tone. Such a phenomenon is commonly observed in clays rich in iron content, where high-temperature exposure promotes the crystallization of hematite phases through iron-oxygen interactions [34].

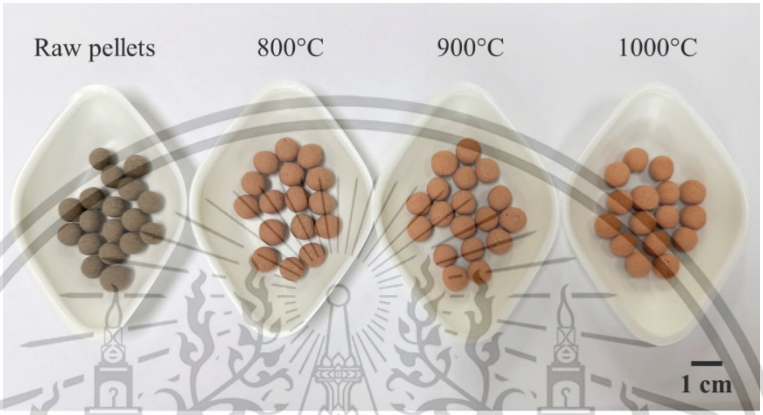

Figure 4.2. The color transformation of EP-LWAs (20 wt.% EP) before and after sintering at 800°C, 900°C, and 1000°C.

The raw pellets measured about 7.86 mm in diameter on average. When sintered at 800 °C, they underwent a modest expansion of 1.45 % to 2.74 %, driven largely by transformations in the red clay, most notably kaolinite dehydroxylation ($Al_2Si_2O_5(OH)_4 \longrightarrow Al_2Si_2O_7 + H_2O$) [35], and the release of structural water, alongside breakdown of organics and carbonates that create small pores. Raising the sintering temperature to 900°C and 1000°C reversed this trend, with diametric shrinkages of 0.25 %–0.97 % and 0.25 %–9.46 % respectively. This contraction reflects densification via particle coalescence and viscous flow mechanisms during sintering, where voids collapse and grains draw together under capillary forces. Expanded perlite (EP), already thermally expanded during its manufacture, did not bloat further at these temperatures; instead, its amorphous silica likely softened and collapsed, contributing to net pellet shrinkage. Concurrently, the melting of feldspar or silica in the clay matrix formed a glassy phase that enhanced overall sintering and further reduced pellet volume.

Figure 4.3 compares the XRD spectra of EP-LWAs with 20 wt.% EP, sintered at 800°C, 900°C, and 1000°C. In all cases, quartz remains the primary crystalline phase, as shown by the strong, stable peak at $2\theta \approx 26.6°$. Feldspar reflections, especially between 27.8° and 28.0°—also persist and grow slightly more intense at higher firing temperatures, implying some recrystallization of the melted glass fraction upon cooling. Conversely, the peaks for kaolinite and illite, which were clear in the raw clay, vanish after sintering above 900°C, signaling their thermal dehydroxylation and transformation into other, non-clay phases. Kaolinite typically converts into metakaolinite by 400–500°C and can further evolve into spinel-type or mullite precursor phases beyond 900°C [36], though no distinct mullite peaks appear—likely due to low abundance or poor crystallinity. Hematite also fails to show unmistakable peaks, perhaps because it is present in very small amounts, or its signals overlap with stronger phases. Overall, the XRD data confirm that sintering breaks down unstable clay minerals while preserving quartz and feldspar, resulting in a more glass-rich, thermally stable microstructure. Samples with different EP loadings exhibit virtually the same pattern of phase changes, underlining a consistent phase-evolution behavior across compositions.

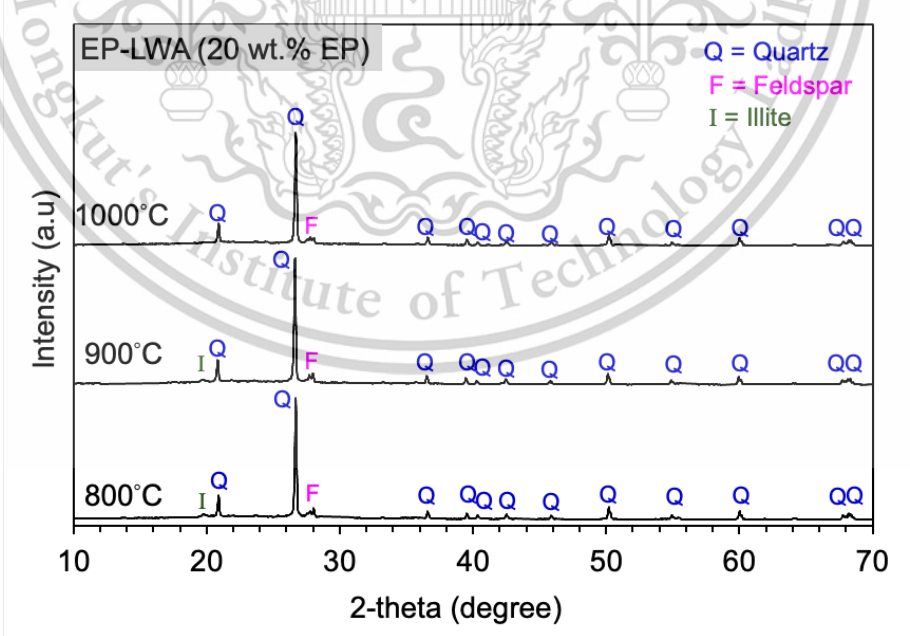

Figure. 4.3. XRD patterns of EP-LWAs containing 20 wt.% EP, sintered at 800°C, 900°C, and 1000°C.

Fig. 4.4 illustrates effect of expanded perlite (EP) content on the bulk density of EP-LWAs sintered at 800°C, 900°C, and 1000°C. Starting with a compact clay-only sample at 0 wt.% EP (about 1.8 g/cm³), adding EP progressively lowers density, reaching 0.9 g/cm³ at 40 wt.% EP. This is due to low intrinsic density and porous nature of EP, which disrupts the overall compactness of aggregate.

Sintering at 1000 °C yields slightly higher densities than at 900°C or 800°C, indicating enhanced densification at elevated temperatures. This likely stems from partial softening and collapse of amorphous silica in EP, which promotes particle consolidation. Nonetheless, regardless of firing temperature, density continually drops with more EP. These findings confirm that incorporating EP effectively lightens LWAs, making them ideal for lightweight applications like horticultural substrates and green roofs.

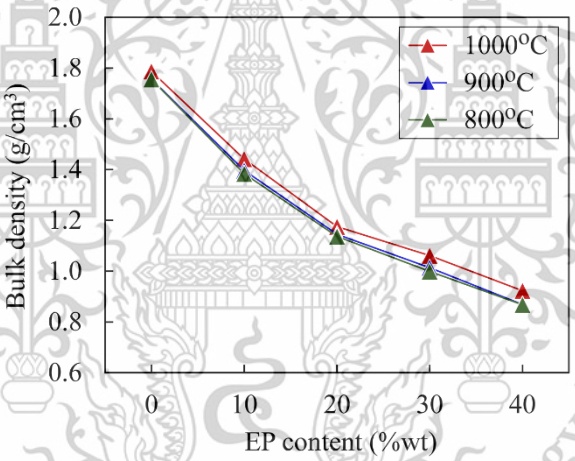

Figure 4.4. Effect of expanded perlite (EP) content on the bulk density of EP-LWAs sintered at 800°C, 900°C, and 1000°C.

Figure 4.5 effect of expanded perlite (EP) content on the porosity of EP-LWAs sintered at 800°C, 900°C, and 1000°C. Pure clay samples (0 wt.% EP) exhibit the lowest porosity (around 33–34%), while specimens with 40 wt.% EP reach approximately 50–53%. This is due to EP porous structure, which introduces extra voids into the ceramic framework. Temperature also influences porosity slightly. Although the upward trend with EP content is consistent, samples fired at 1000 °C show marginally lower porosity than those sintered at 800°C or 900°C. This small decrease likely results from partial softening and densification of EP particles at higher temperatures, causing some pore

collapse. Conversely, at 800°C and 900°C, EP retains its structure better, preserving more porosity.

The observed rise in bulk density and slight drop in porosity at 1000°C stem from intensified sintering densification typical of ceramics. At this elevated temperature, feldspar and silica components within the red clay and expanded perlite begin to soften, triggering partial vitrification. This softening promotes viscous flow, neck growth between particles, and grain-boundary diffusion, causing minor pore closure. In these experiments, the expanded perlite—which had already been thermally bloated during manufacture—does not re-expand; instead, it softens and collapses under heat, further reducing open porosity. Although this enhanced densification boosts the mechanical strength of EP-LWAs, it can slightly impair their water-holding capability—an essential trait for horticultural uses. Therefore, a balance must be struck between mechanical robustness and functional porosity.

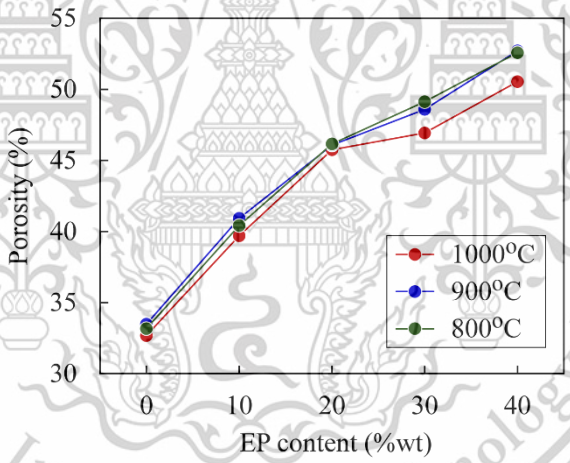

Figure 4.5. Effect of expanded perlite (EP) content on the porosity of EP-LWAs sintered at 800°C, 900°C, and 1000°C.

Figure 4.6 shows effect of expanded perlite (EP) content on the water absorption of EP-LWAs sintered at 800°C, 900°C, and 1000°C. The water absorption in EP-LWAs increases linearly with higher expanded perlite (EP) content, regardless of sintering temperature. Pure clay samples (0 wt.% EP) absorb the least water (around 18–19%) because of their denser structure. As EP proportion rises, water uptake climbs steadily, peaking at roughly 55–61% for 40 wt.% EP, due to naturally porous framework of EP that adds extra voids for water retention. Sintering temperature slightly affects

absorption in which specimens fired at 1000°C hold marginally less water than those sintered at 900°C or 800°C. This slight drop is likely due to increased densification and partial collapse of pores at higher heat, which reduces interconnected pathways for water. Nonetheless, across all temperatures, more EP consistently yields greater water absorption.

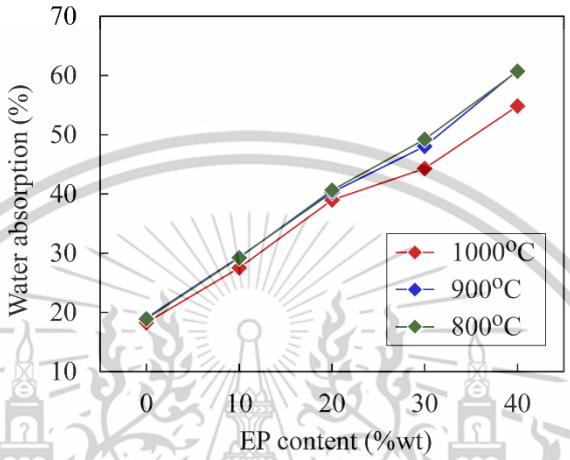

Figure 4.6. Effect of expanded perlite (EP) content on the water absorption of EP-LWAs sintered at 800°C, 900°C, and 1000°C.

The selection of optimal sintering temperature and expanded perlite (EP) proportion for NPK loading requires balancing porosity, mechanical strength, and energy efficiency. High porosity ensures effective fertilizer uptake and retention, while adequate strength keeps the aggregates intact during handling. Lower energy usage also supports sustainable production. The data show that higher EP content increases both porosity and water absorption, enhancing fertilizer-loading potential. However, excessive EP (30–40 wt.%) compromises pellet strength, making them brittle. On the other hand, 20 wt.% EP achieves an optimal compromise—providing enough porosity for nutrient storage without sacrificing structural integrity.

Sintering temperature critically influences the final properties of lightweight aggregates. At 800 °C, LWAs display maximum porosity and water uptake but lack sufficient mechanical strength due to limited densification. Conversely, firing at 1000°C enhances strength via greater densification but decreases porosity and water absorption, reducing fertilizer-loading effectiveness and consuming more energy. In this study, 900°C was identified as the optimal temperature, balancing porosity, structural

stability, and energy efficiency. Lowering the firing temperature from the conventional 1000–1300°C range to 900°C notably reduces thermal energy requirements and carbon emissions. Producing porous EP-LWAs with desirable properties at 900°C thus offers a more sustainable, energy-saving route. Additionally, using waste-derived expanded perlite as a pore-forming agent improves the environmental footprint by valorizing waste and lowering reliance on costly raw materials. Accordingly, for NPK incorporation, EP-LWAs with 20 wt.% EP sintered at 900 °C were chosen, exhibiting a bulk density of 1.2 g/cm³, porosity of 46.1%, and water absorption of 40.3%.

The physical characteristics of the optimized EP-LWAs developed in this study were benchmarked against three widely used commercial lightweight aggregates in horticulture, as shown in Table 4.2. The EP-LWAs had a slightly smaller average diameter (8.16 mm) than the commercial counterparts (9.02–9.31 mm), which may be advantageous for applications that require finer particle sizes. Regarding bulk density, the EP-LWAs showed considerably higher values (1.15 g/cm³) than the commercial alternatives (0.56–0.68 g/cm³), implying greater mechanical durability—an asset in green roofing or vertical planting systems where structural support is crucial. Although their porosity (46.1%) and water absorption (40.3%) were somewhat lower than the highest values observed in commercial products (up to 53.0% porosity and 94.9% absorption), these values remain within functional limits for horticultural use. Importantly, the moderate water absorption level of EP-LWAs offers sufficient moisture retention while avoiding waterlogging [37], which is beneficial in systems with controlled irrigation, where effective water regulation is essential for plant vitality.

Table 4.2. Comparison of physical properties between EP-LWAs developed in this study and commercially available LWAs used in horticulture.

Samples	Average diameter (mm)	Bulk density (g/cm^3)	Porosity (%)	Water absorption (%)
Commercial LWA no.1	9.31	0.56	53.0	94.9
Commercial LWA no.2	9.25	0.68	43.8	64.6
Commercial LWA no.3	9.02	0.56	49.5	88.1
EP-LWA (20 wt%EP)	8.16	1.15	46.1	40.3

4.3 Analysis of fertilizer in NPK-incorporated LWAs

4.3.1 Evaluation of Alternative Fertilizer Absorbing media

In this study, alternative substances including glycerol and vegetable oil—were evaluated as potential fertilizer-absorbing media in comparison to the conventional absorbent, carboxymethyl cellulose (CMC). The procedure for incorporating fertilizers into the lightweight aggregates (LWAs) is detailed in Section 3.3. A ratio of 30 g of fertilizer powder per 100 mL of absorbing medium was used in this process. Following the incorporation process, the primary nutrient loading was analyzed, with the results presented in Table 4.3.

Table 4.3 Analysis of NPK nutrients in EP-LWAs using different absorbing media.

Absorbing media	Nutrients		
	N (%)	P (%)	K (%)
Glycerol	0.6	<0.5	0.6
Vegetable Oil	<0.5	undetectable	<0.15
CMC	1.3	1.1	1.4

Glycerol was initially selected due to its viscous, gel-like nature, which appeared similar to CMC in physical form. However, experimental results revealed its unsuitability. When mixed with powdered NPK fertilizer, glycerol did not form a homogenous solution. Phase separation occurred, and the fertilizer particles remained partially undissolved. During the vacuum infiltration process, minimal air was observed escaping from the LWA pellets, indicating ineffective replacement of air within the pores. Post-infiltration analysis of the fertilizer content in the LWA pellets showed insufficient nutrient loading: N at 0.6%, P below 0.5%, and K at 0.6%. These results were deemed unsatisfactory, prompting the exploration of alternative materials.

Vegetable oil was also tested due to its high viscosity, which was hypothesized to aid in surface adhesion and absorption. However, upon mixing, the oil failed to blend with the powdered fertilizer, instead forming a coating layer on the surface of the LWA pellets. This coating not only prevented the fertilizer solution from penetrating into the internal pores but also caused pore blockage. During vacuum treatment, no visible air bubbles were observed, implying poor infiltration.

Furthermore, an unpleasant rancid odor developed in the pellets after treatment, raising concerns about potential soil toxicity. Nutrient analysis revealed extremely low fertilizer retention: N below 0.5%, P is undetectable, and K below 0.15%.

CMC was employed as the standard absorbing medium due to its well-documented gel-forming properties and compatibility with various hydrophilic substances. In contrast to glycerol and vegetable oil, CMC demonstrated superior performance in terms of fertilizer incorporation and nutrient retention. When mixed with powdered NPK fertilizer, CMC formed a stable and homogeneous gel without any observable phase separation. During the vacuum infiltration process, significant air displacement was observed from the LWA pellets, indicating effective penetration of the fertilizer gel into the pore structure. Post-infiltration nutrient analysis confirmed high levels of nutrient retention within the LWA pellets, with N content at 1.3%, P at 1.1%, and K at 1.4%. These values represent the highest loading efficiencies among the tested media and affirm the suitability of CMC for applications requiring effective nutrient delivery via LWA systems.

4.3.2 Microstructure and chemical analysis of NPK-incorporated LWA

A 50 wt.% NPK-incorporated LWA specimen was selected for analysis of nutrient distribution. Cross-sectional micrographs of the fertilizer-impregnated aggregates and their corresponding energy-dispersive X-ray spectroscopy (EDS) elemental distribution maps—differentiating the clay- region, and EP region domains—are presented in Figures 4.7 and 4.8, respectively. Quantitative compositional data for each domain is shown in Table 4.4, enabling a comparative assessment of nutrient localization within phase microstructure.

LWAs compositions are dominated by oxygen (O), silicon (Si), and aluminum (Al), reflecting their silicate, aluminosilicate, and oxide framework. The expanded perlite regions show a slightly higher Si content (25.14%) than the clay domains (21.61%), consistent with volcanic glass nature of perlite. High carbon (C) levels in both areas (9.51% in expanded perlite and 11.61% in clay) stem from the use of carbon-rich carboxymethyl cellulose (CMC) as a fertilizer-absorbing agent. Iron (Fe) is more abundant in the clay (2.44%) than in the expanded perlite (1.44%), indicating that Fe is more prevalent within the natural clay matrix.

Potassium (K) and phosphorus (P), which are key macronutrients in NPK fertilizer, were clearly detected in both the clay-rich and expanded perlite-rich regions of the porous LWAs, confirming that the fertilizer was successfully incorporated into the internal structure of the aggregates. Quantitative analysis using energy-dispersive X-ray spectroscopy (EDS) showed that the perlite-rich areas had a higher K content (3.33 wt%) compared to the clay-rich areas (2.12 wt%). This suggests that the highly connected pore network of expanded perlite allows for better physical trapping and retention of potassium ions (K^+), which are known to be highly mobile. On the other hand, P was found in higher amounts in the clay matrix (0.79 wt%) than in the expanded perlite areas (0.27 wt%). This difference indicates that the clay structure, particularly its aluminosilicate layers and surfaces containing iron and aluminum oxides or hydroxides, has a stronger chemical attraction to phosphate ions, allowing more phosphorus to be retained in the clay phase.

The expanded perlite component, which consists of a glass-like silicate structure, contains a wide range of pore sizes from submicron to micron scale. These pores help retain dissolved nutrients mainly through physical adsorption (physisorption) within the pore spaces [38]. Previous studies have shown that glassy silicates like perlite can sometimes hold more nutrients than materials that rely on typical ion-exchange mechanisms. This is due to the role of weak intermolecular forces, such as van der Waals interactions, and capillary action in trapping nutrients. In contrast, the clay minerals, which are rich in iron (Fe) and aluminum (Al), have surface hydroxyl and oxide groups that can form stronger chemical bonds with phosphate ions [39]. These surfaces allow for both inner-sphere complexation (direct bonding) and electrostatic attraction, making the clay phase more effective at chemically binding phosphate nutrients [39].

The EDS elemental mapping results confirmed that potassium (K) and phosphorus (P) were evenly distributed throughout the two types of pores in the LWAs. However, nitrogen (N) could not be detected using standard EDS analysis. This is because nitrogen has a low atomic number and produces very weak X-ray signals, making it difficult to detect with this technique.

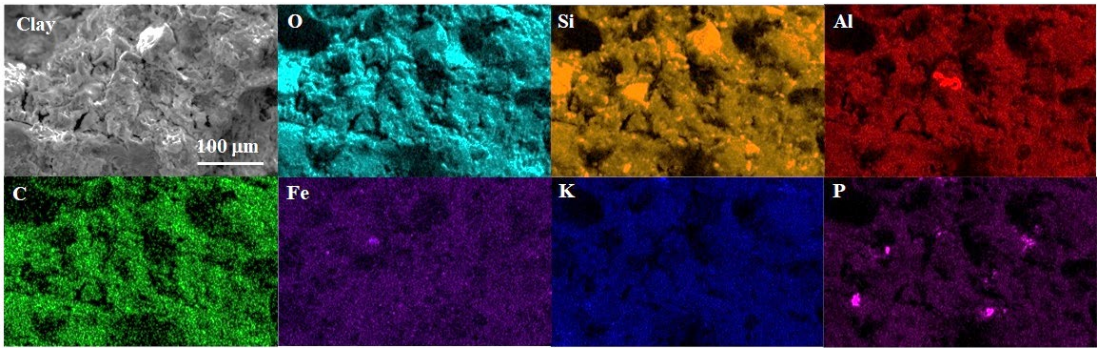

Figure 4.7. SEM image of the cross-section of NPK-incorporated LWA in clay region with EDS mapping showing composition and distribution of key elements.

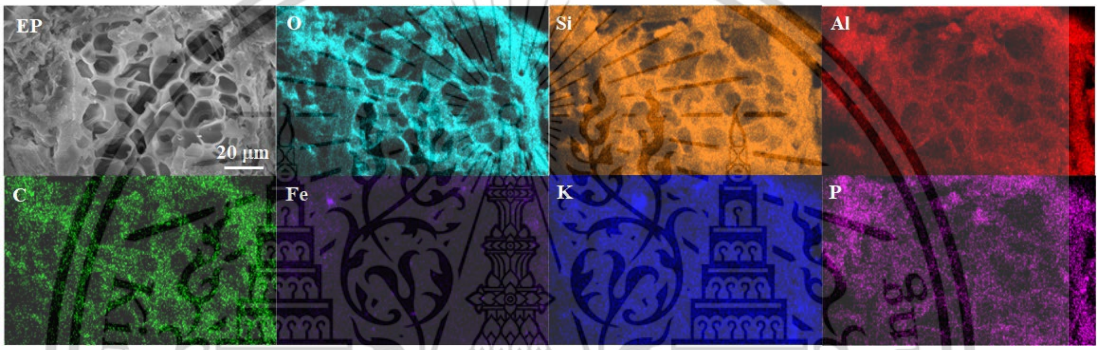

Figure 4.8. SEM image of the cross-section of NPK- incorporated LWA in EP region with EDS mapping showing composition and distribution of key elements.

Table 4.4. The EDS analysis of each element in NPK-incorporated LWA.

Elements (wt%)	O	Si	Al	C	Fe	K	P
Clay	46.21	21.61	7.36	11.61	2.44	2.12	0.79
EP	46.16	25.14	6.64	9.51	1.44	3.33	0.27

The nutrient content of NPK fertilizer in the expanded perlite lightweight aggregates (EP-LWAs) was measured following the Thai Standard Method for Chemical Fertilizer Analysis [25]. This method evaluates the total amounts of nitrogen (N), phosphorus (P), and water-soluble potassium (K). As shown in Table 4.5, the amount of nutrients retained in the aggregates increased steadily with higher amounts of fertilizer added. For example, EP-LWA samples with 30 wt.% fertilizer (F30) contained 1.3% N, 1.1% P, and 1.4% K. When the fertilizer content was increased to 40 wt.% (F40), the levels rose to 1.9% N, 1.5% P, and 2.1% K. The highest levels were found in

the samples with 50 wt.% fertilizer (F50), which contained 2.2% N, 1.8% P, and 2.9% K. These results clearly show that increasing the fertilizer content improves the amount of macronutrients retained in the porous structure of the aggregates. Among the three nutrients, potassium was present in the highest amount, indicating that the material effectively holds the water-soluble K^+ ions, which are important for plant uptake. Phosphorus levels also increased in proportion to the added fertilizer, suggesting it may be released gradually over time. In contrast, nitrogen levels were lower, likely because some of it was lost during the preparation process due to its higher tendency to evaporate.

Soil fertility is commonly assessed based on the levels of key macronutrients, namely total nitrogen (N), extractable phosphorus (P), and extractable potassium (K). According to Thailand's national soil fertility standards [40], nitrogen levels below 0.1% are considered low, between 0.1% and 0.2% are considered medium, and above 0.2% are considered high. For phosphorus, concentrations below 10 mg/kg are classified as low, 10–25 mg/kg as medium, and above 25 mg/kg as high. Similarly, potassium levels are considered low if they are below 60 mg/kg, medium between 60–90 mg/kg, and high if they exceed 90 mg/kg. These benchmarks are widely used to evaluate the nutrient status of soil in both agricultural and environmental studies.

When benchmarked against these classifications, NPK-loaded EP-LWAs highly exceed the "high" thresholds of natural soils: total N spans 1.3–2.2%, extractable P ranges from 11,000 to 18,000 mg/kg, and extractable K extends from 14,000 to 29,000 mg/kg, orders of magnitude above the respective soil fertility cutoffs. Consequently, EP-LWAs represent exceptionally rich sources of N, P, and K.

Moreover, Thai Organic Fertilizer Standards (TAS 9503-2005) for compost [41] mandate minimum concentrations of ≥1.0% N, ≥0.5% P_2O_5, and ≥0.5% K_2O. NPK-incorporated EP-LWAs comfortably surpass these requirements: N content of 1.3–2.2%, P_2O_5 of 1.1–1.7%, and K_2O of 1.4–2.9%. These results confirm the suitability EP-LWAs as high-performance, nutrient-rich substrates for horticultural and agricultural use.

The nutrient of NPK-loaded EP-LWAs were benchmarked against common organic amendments such as cow manure, pig manure, rice straw, and cassava stems, as detailed in Table 4.5. EP-LWAs exhibited markedly higher concentrations of the primary macronutrients (N, P, K) than most conventional organic fertilizers. Notably,

EP-LWAs deliver a more balanced and elevated NPK ratio, with phosphorus and potassium levels that typically limit soil fertility. Thus, EP-LWAs emerge as a compelling alternative or supplementary amendment for enhancing soil nutrient status in sustainable agricultural systems and urban horticulture.

Table 4.5. Comparison of NPK nutrients in EP-LWAs with the NPK content in various types of organic fertilizers.

Samples		Nutrients		
		N (%)	P (%)	K (%)
This study	EP-LWA-F30	1.3	1.1	1.4
	EP-LWA-F40	1.9	1.5	2.1
	EP-LWA-F50	2.2	1.8	2.9
Organic fertilizers [40]	Cow manure	1.1	0.40	1.60
	Pig manure	1.3	2.40	1.00
	Rice straw	0.59	0.08	0.26
	Cassava stem	1.23	0.24	1.23

4.3.3 Preliminary study of fertilizer release behavior

A preliminary release study was conducted using the EP-LWA sample loaded with 50 wt.% fertilizer (EP LWAs-F50) to evaluate the nutrient release profile under static soaking conditions. Electrical conductivity (EC) measurements were used to indirectly estimate the cumulative amount of fertilizer released over time. A calibration curve was established between fertilizer concentration and EC, resulting in a linear relationship with a high degree of correlation as shown in Figure 4.9. The regression equation obtained was:

$$EC\ (mS/cm) = 12.467 \times Fertilizer\ (g) \quad (4.1)$$

This equation was subsequently used to convert EC measurements to cumulative fertilizer release at each time interval.

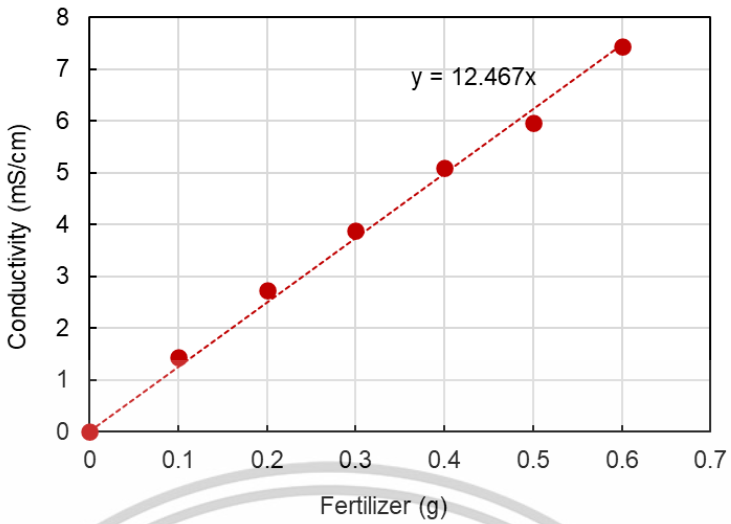

Figure 4.9. Calibration curve of linear relationship between fertilizer concentration and electrical conductivity (EC).

The release profile of EP LWAs-F50, as illustrated in the cumulative release (%) graph in Figure 4.10, exhibited a typical biphasic pattern commonly associated with diffusion-controlled systems. In the early stage (0–9 h), a sharp increase in release was observed, reaching approximately 53.6% of the total fertilizer load. This phase is attributed to the rapid diffusion of readily available surface-bound nutrients and those in larger, more accessible pores. Beyond this point, the release rate slowed progressively, with the cumulative release reaching 66.6% at 12 h and 78.5% at 24 h. The release curve began to stable at 48 h (≈89.6%) and approached completion at 168 h, reaching 100% total release. This sustained release pattern indicates that the porous structure of EP LWAs facilitates gradual nutrient diffusion, particularly from smaller pores. Furthermore, the sharp initial release phase suggests that part of the fertilizer may be weakly retained or located near the surface, leading to an early burst release.

The fertilizer release behavior of the EP LWAs-F50 formulation was evaluated in comparison with the criteria established by the European Standardization Committee (CEN) for slow-release fertilizers (SRFs). According to CEN guidelines, a fertilizer may be classified as slow-release if it satisfies the following three conditions under standardized conditions at 25 °C: (1) no more than 15% of the nutrients are released within the first 24 h, (2) no more than 75% of the total nutrients are released

within 28 days, and (3) at least approximately 75% of the nutrients are ultimately released within the specified release period. In the present study, the EP LWAs-F50 sample exhibited a rapid nutrient release pattern, with approximately 78.5% of the fertilizer released within the first 24 h and complete release (100%) achieved by 168 h (7 days). Although the system meets the third criterion regarding total nutrient release, the first two criteria were not fulfilled, indicating that the release rate is too rapid for the material to be classified as a standard SRF.

To achieve compliance with the CEN classification for slow-release systems, further formulation modifications are required. Several strategies are recommended to retard the release rate, particularly during the initial 24-hour period. These include applying an additional coating layer using biodegradable polymers such as polylactic acid (PLA) or natural polymers like alginate and starch to create a diffusion barrier. Modifying the absorbing media by enhancing the viscosity or crosslinking density of the carboxymethyl cellulose (CMC) gel could also slow nutrient migration. Furthermore, altering the pore structure of the LWAs to reduce open porosity or sealing the surface may limit rapid nutrient diffusion. Incorporating commercial encapsulated fertilizers or blending with coated NPK granules may offer a hybrid approach that balances immediate and sustained nutrient availability. Finally, extending the drying or curing time following fertilizer loading may promote stronger nutrient–matrix interactions, thereby reducing the initial burst release.

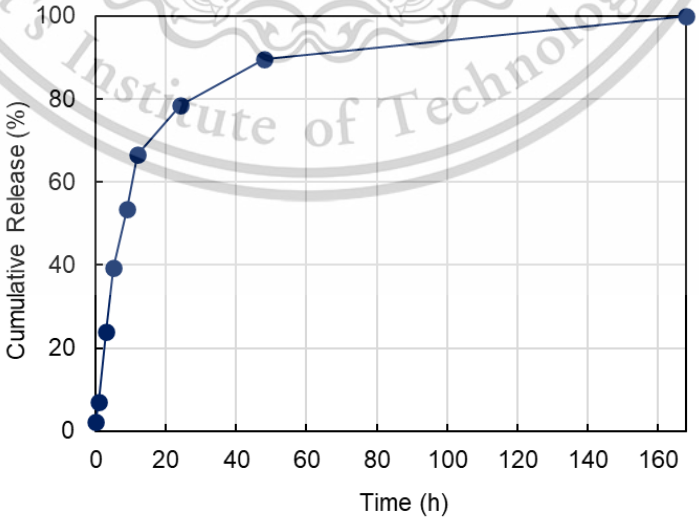

Figure 4.10. The cumulative release profile of fertilizer from EP LWAs-F50 as a function of time under static soaking conditions.

Chapter 5

Conclusion

This study successfully developed and comprehensively characterized expanded perlite-based lightweight aggregates (EP-LWAs) incorporated with NPK fertilizer, underscoring their potential application in sustainable agriculture and horticulture. Through the optimization of sintering parameters, a temperature of 900 °C was identified as the most appropriate for producing EP-LWAs with desirable physical properties, namely a bulk density of 1.15 g/cm³, porosity of 46.09%, and water absorption of 40.28%. These attributes render the EP-LWAs highly suitable for use in green roofs, vertical gardens, and as soil amendment materials due to their lightweight nature and effective nutrient retention capacity.

Nutrient analysis revealed that EP-LWAs loaded with 50 wt.% fertilizer contained 2.2% nitrogen (N), 1.8% phosphorus (P), and 2.9% potassium (K). These concentrations not only exceed the average NPK levels typically found in Thai agricultural soils but also surpass the minimum thresholds specified by national compost fertilizer standards. Such results underscore the potential of EP-LWAs as highly efficient nutrient carriers, offering a more concentrated and balanced nutrient profile compared to conventional organic fertilizers such as manure or crop residues. In addition, the integration of fertilizer within the porous matrix of EP-LWAs facilitates nutrient encapsulation, which may reduce leaching losses and enhance the availability of nutrients over an extended period.

Preliminary release studies of EP-LWAs-F50 demonstrated a rapid nutrient release pattern, with over 78% of the total nutrient content released within the first 24 h and complete release achieved by 168 h. While this behavior indicates effective nutrient transfer, it does not meet the release rate criteria defined by the European Standardization Committee (CEN) for classification as a slow-release fertilizer. To align the release kinetics with international standards, future studies should explore structural and compositional modifications to retard nutrient diffusion. These may

include the application of biodegradable polymer coatings, adjustment of pore architecture, incorporation of cross-linked hydrogel matrices, or blending with coated fertilizer granules. Furthermore, extended drying periods after fertilizer incorporation may promote stronger nutrient retention within the matrix.

References

[1] Matthew R. Hall, Materials for Energy Efficiency and Thermal Comfort in Buildings, Woodhead Publishing Series in Energy, 2010. https://books.google.co.th/books?hl=th&lr=&id=CohwAgAAQBAJ&oi=fnd&pg=PP1&ots=y_KaXqrQq3&sig=P-WsgejXMEZIlRdqLDPp5Akn49w&redir_esc=y#v=onepage&q&f=false (accessed May 30, 2023).

[2] A.M. Rashad, Lightweight expanded clay aggregate as a building material – An overview, Constr Build Mater. 170 (2018) 757–775. https://doi.org/10.1016/J.CONBUILDMAT.2018.03.009.

[3] G.A.G.B.A.B.J.M. M.G. Alexander, Engineering and Transport Properties of the Interfacial Transition Zone in Cementitious Composites, RILEM Publications. (1999). https://books.google.co.th/books?hl=th&lr=&id=M2laPRjXOe0C&oi=fnd&pg=PR13&ots=ftg1J4RWOp&sig=vZQwhHb6s_S5ncCES7NG6HIcmn4&redir_esc=y#v=onepage&q=LECA&f=false (accessed May 30, 2023).

[4] A. Ozguven, L. Gunduz, Examination of effective parameters for the production of expanded clay aggregate, Cem Concr Compos. 34 (2012) 781–787. https://doi.org/10.1016/J.CEMCONCOMP.2012.02.007.

[5] T. Shichi, K. Takagi, Clay minerals as photochemical reaction fields, Journal of Photochemistry and Photobiology C: Photochemistry Reviews. 1 (2000) 113–130. https://doi.org/10.1016/S1389-5567(00)00008-3.

[6] M. Malakootian, J. Nouri, H. Hossaini, Removal of heavy metals from paint industry's wastewater using Leca as an available adsorbent, International Journal of Environmental Science and Technology. 6 (2009) 183–190. https://doi.org/10.1007/BF03327620/METRICS.

[7] A. Dordio, A.J.P. Carvalho, Constructed wetlands with light expanded clay aggregates for agricultural wastewater treatment, Science of The Total Environment. 463–464 (2013) 454–461. https://doi.org/10.1016/J.SCITOTENV.2013.06.052.

[8] S. Sharifnia, M.A. Khadivi, T. Shojaeimehr, Y. Shavisi, Characterization, isotherm and kinetic studies for ammonium ion adsorption by light expanded clay

aggregate (LECA), Journal of Saudi Chemical Society. 20 (2016) S342–S351. https://doi.org/10.1016/J.JSCS.2012.12.003.

[9] E.M. Kalhori, K. Yetilmezsoy, N. Uygur, M. Zarrabi, R.M.A. Shmeis, Modeling of adsorption of toxic chromium on natural and surface modified lightweight expanded clay aggregate (LECA), Appl Surf Sci. 287 (2013) 428–442. https://doi.org/10.1016/J.APSUSC.2013.09.175.

[10] K. Laursen, T.J. White, D.J.F. Cresswell, P.J. Wainwright, J.R. Barton, Recycling of an industrial sludge and marine clay as light-weight aggregates, J Environ Manage. 80 (2006) 208–213. https://doi.org/10.1016/J.JENVMAN.2005.08.026.

[11] M. Guo, M. Liu, F. Zhan, L. Wu, Preparation and Properties of a Slow-Release Membrane-Encapsulated Urea Fertilizer with Superabsorbent and Moisture Preservation, Ind Eng Chem Res. 44 (2005) 4206–4211. https://doi.org/10.1021/IE0489406.

[12] E. Trenkel and Dr. Martin, Improving Fertilizer Use Efficiency, IFA,International Fertilizer Industry Association, 1997. http://www.wnkgroup.com/Controlled-Release%20fertilizer%20in%20Agriculture.pdf (accessed May 31, 2023).

[13] G.M. Blouin, D.W. Rindt, O.E. Moore, Sulfur-Coated Fertilizers for Controlled Release: Pilot Plant Production, J Agric Food Chem. 19 (1971) 801–808. https://doi.org/10.1021/JF60177A039/ASSET/JF60177A039.FP.PNG_V03.

[14] M.H. Sazzad, Md.T. Islam, F. Chowdhury, A Review & Outlook of Slow-Release Fertilizer A breakthrough product for agronomy & horticulture, (n.d.). https://www.researchgate.net/publication/318135291_A_Review_Outlook_of_Slow-Release_Fertilizer_A_breakthrough_product_for_agronomy_horticulture (accessed June 1, 2023).

[15] Controlled-Release Fertilizers - Garden.org, (n.d.). https://garden.org/learn/articles/view/698/Controlled-Release-Fertilizers/ (accessed June 14, 2023).

[16] L.S. Liu, J. Kost, M.L. Fishman, K.B. Hicks, A review: Controlled release systems for agricultural and food applications, ACS Symposium Series. 992 (2008) 265–281. https://doi.org/10.1021/BK-2008-0992.CH014.

[17] C. Varadachari, Slow-release and Controlled-release Nitrogen Fertilizers, (2010). https://www.researchgate.net/publication/262839872 (accessed June 1, 2023).

[18] C.H. Peacock, J.M. DiPaola, Bermudagrass Response to Reactive Layer Coated Fertilizers, Agron J. 84 (1992) 946–950. https://doi.org/10.2134/AGRONJ1992.00021962008400060007X.

[19] P. V. Nelson, Greenhouse operation and management., Greenhouse Operation and Management. (1991).

[20] M.E. Trenkel, Slow-and controlled-release and stabilized fertilizers: An option for enhancing nutrient use efficiency in agriculture in agriculture, in: International Fertilizer Industry Association (IFA), Paris, France, 2010. https://scholar.google.com/scholar_lookup?hl=th-TH&publication_year=2010&pages=%00empty%00&author=M.+E.+Trenkel&isbn=%00null%00&title=Slow-and+controlled-release+and+stabilized+fertilizers%3A+An+option+for+enhancing+nutrient+use+efficiency+in+agriculture+in+agriculture (accessed May 31, 2023).

[21] Ministry of Agriculture and Cooperative, Notification of the Ministry of Agriculture and Cooperative Re: Prescribing the Method of Analysis of Chemical Fertilizer B.E. 2559, Bangkok, Thailand, 2559. https://siweb.dss.go.th/index.php/th/registration-form/4636-2559-5 (accessed May 31, 2023).

[22] C.W. Du, J.M. Zhou, A. Shaviv, Release Characteristics of Nutrients from Polymer-coated Compound Controlled Release Fertilizers, J Polym Environ. 14 (2006) 223–230. https://doi.org/10.1007/S10924-006-0025-4.

[23] A. Olad, H. Zebhi, D. Salari, A. Mirmohseni, A. Reyhani Tabar, Slow-release NPK fertilizer encapsulated by carboxymethyl cellulose-based nanocomposite with the function of water retention in soil, Materials Science and Engineering: C. 90 (2018) 333–340. https://doi.org/10.1016/J.MSEC.2018.04.083.

[24] A. Rashidzadeh, A. Olad, Slow-released NPK fertilizer encapsulated by NaAlg-g-poly(AA-co-AAm)/MMT superabsorbent nanocomposite, Carbohydr Polym. 114 (2014) 269–278. https://doi.org/10.1016/J.CARBPOL.2014.08.010.

[25] K. Rop, G.N. Karuku, D. Mbui, I. Michira, N. Njomo, Formulation of slow release NPK fertilizer (cellulose-graft-poly(acrylamide)/nano-hydroxyapatite/soluble fertilizer) composite and evaluating its N mineralization potential, Annals of Agricultural Sciences. 63 (2018) 163–172. https://doi.org/10.1016/J.AOAS.2018.11.001.

[26] X. Zhang, Y. Liu, P. Lu, M. Zhang, Preparation and properties of hydrogel based on sawdust cellulose for environmentally friendly slow-release fertilizers, Green Processing and Synthesis. 9 (2020) 139–152. https://doi.org/10.1515/GPS-2020-0015/ASSET/GRAPHIC/J_GPS-2020-0015_FIG_013.JPG.

[27] R.A. Ramli, Y.M. Lian, N.M. Nor, N.I.Z. Azman, Synthesis, characterization, and morphology study of coco peat-grafted-poly(acrylic acid)/NPK slow release fertilizer hydrogel, Journal of Polymer Research. 26 (2019) 1–7. https://doi.org/10.1007/S10965-019-1952-9/METRICS.

[28] M.D. Gumelar, M. Hamzah, A.S. Hidayat, D.A. Saputra, Idvan, Utilization of Chitosan as Coating Material in Making NPK Slow Release Fertilizer, Macromol Symp. 391 (2020). https://doi.org/10.1002/MASY.201900188.

[29] W. Pang, D. Hou, H. Wang, S. Sai, B. Wang, J. Ke, G. Wu, Q. Li, M.T. Holtzapple, Preparation of Microcapsules of Slow-Release NPK Compound Fertilizer and the Release Characteristics, J Braz Chem Soc. 29 (2018) 2397–2404. https://doi.org/10.21577/0103-5053.20180117.

[30] A.S.M. Ghumman, R. Shamsuddin, M.M. Nasef, W.Z.N. Yahya, A. Abbasi, H. Almohamadi, Sulfur enriched slow-release coated urea produced from inverse vulcanized copolymer, Science of the Total Environment. 846 (2022). https://doi.org/10.1016/J.SCITOTENV.2022.157417.

[31] E.H. Boutriouia, T. El Assimi, M. Raihane, R. Beniazza, H. Ben Youcef, M. Khouloud, M.H. V. Baouab, A. El Kadib, M. Lahcini, Polymethyl methacrylate-g-carboxy-methylcellulose as an amphiphilic coating material for slow-release fertilizer, Prog Org Coat. 172 (2022). https://doi.org/10.1016/J.PORGCOAT.2022.107102.

[32] ASTM C20; Standard Test Methods for Apparent Porosity, Water Absorption, Apparent Specific Gravity, and Bulk Density of Burned Refractory Brick and Shapes by Boiling Water. ASTM International: West Conshohocken, PA, USA, 2022.

[33] Notification of the Ministry of Agriculture and Cooperatives of Thailand; Re. Prescribing the Method of Analysis of Chemical fertilizers B.E. 2559. https://www.doa.go.th/ard/wp-content/uploads/2019/11/FEMOA13.pdf (accessed 3 February 2025).

[34] J. Carneiro, D.M. Tobaldi, W. Hajjaji, M.N. Capela, R.M. Novais, M.P. Seabra, J.A. Labrincha, Red mud as a substitute coloring agent for the hematite pigment, Ceram. Int. 44 (2018) 4211–4219. https://doi.org/10.1016/J.CERAMINT.2017.11.225.

[35] Y. Cheng, J. Xing, C. Bu, J. Zhang, G. Piao, Y. Huang, H. Xie, X. Wang, Dehydroxylation and structural distortion of kaolinite as a high-temperature sorbent in the furnace, Minerals. 9 (2019) 587. https://doi.org/10.3390/MIN9100587.

[36] M. Abubakar, A. Muthuraja, D.K. Rajak, N. Ahmad, C.I. Pruncu, L. Lamberti, A. Kumar, Influence of Firing Temperature on the Physical, Thermal and Microstructural Properties of Kankara Kaolin Clay: A Preliminary Investigation, Materials. 13 (2020) 1872. https://doi.org/10.3390/MA13081872.

[37] M.I. Aoda, A.J.M. Smucker, S.S. Majeed, H.A. Mohammed, F.H. Al-Sahaf, G.P. Robertson, Novel root zone soil water retention improves production with half the water in arid sands, Agron. J. 113 (2021) 2398–2406. https://doi.org/10.1002/agj2.20648.

[38] Interaction of Perlite with Fertilizer Nutrients in Different Soil Types. https://www.perlite.org/wp-content/uploads/2024/11/Perlite-and-Fertilizer-Nutrients.pdf. (accessed April 21, 2025).

[39] G.K. Kome, R.K. Enang, F.O. Tabi, B.P.K. Yerima, G.K. Kome, R.K. Enang, F.O. Tabi, B.P.K. Yerima, Influence of Clay Minerals on Some Soil Fertility Attributes: A Review, Open J. Soil Sci. 9 (2019) 155–188. https://doi.org/10.4236/OJSS.2019.99010.

[40] T. Nyi, V. Philip, M.I.B.H. Bujang, K. Ra, B. Irianta, P. Sengxua, N. Sipaseuth, A.A. Harirah, B. Bin Jantan, S.M. Salguero, P. Meunchang, V.M. Quyet, N.Q. Hai, P. Moody, T.E. Jäkel, W. Soda, 2017. ASEAN Guidelines on soil and nutrient management, first ed., Deutsche Gesellschaft für Internationale Zusammenarbeit (GIZ) GmbH, Germany. [Online ebook]. ISBN: 978-616-445-746-1.

[41] Notification of Thai National Committee on Agricultural Commodity and Food Standards, Subject: Thai Agricultural Commodity and Food Standards: Compost (TAS 9503-2005). https://faolex.fao.org/docs/pdf/tha201747.pdf. (accessed 21 February 2024).

Appendix

Open Ceramics 22 (2025) 100790

Contents lists available at ScienceDirect

Open Ceramics

journal homepage: www.sciencedirect.com/journal/open-ceramics

Fabrication and characterization of lightweight aggregates with expanded perlite and NPK nutrient incorporation

Panadda Rungrueng [a], Montree Hankoy [a], Mettaya Kitiwan [a,b,*], Nittaya Keawprak [c], Phacharaphon Tunthawiroon [d]

[a] Department of Physics, School of science, King Mongkut's Institute of Technology Ladkrabang, Bangkok, 10520, Thailand
[b] Devices and System for Energy and Environment Research Unit, King Mongkut's Institute of Technology Ladkrabang, Bangkok, 10520, Thailand
[c] Thailand Institute of Scientific and Technological Research, Pathum Thani, 12120, Thailand
[d] Department of Industrial Engineering, School of Engineering, King Mongkut's Institute of Technology Ladkrabang, Bangkok, 10520, Thailand

ARTICLE INFO

Keywords:
Lightweight aggregates
NPK nutrients
Planting materials

ABSTRACT

This study focuses on the development of porous lightweight aggregates incorporated with NPK fertilizer as a sustainable nutrient carrier for agricultural applications. The integration of expanded perlite (EP) as a pore-forming agent enabled the production of lightweight aggregates (EP-LWAs) at lower sintering temperatures (900 °C) while maintaining high porosity and water absorption properties, reducing energy consumption compared to conventional high-temperature ceramic processing. The optimized EP-LWAs exhibited a bulk density of 1.15 g/cm^3, porosity of 46.09 %, and water absorption of 40.28 %, ensuring enhanced nutrient retention capacity. The fertilizer incorporation process was achieved using a simple vacuum infiltration technique, effectively loading the pellets with 1.2 % nitrogen (N), 2.6 % phosphorus (P), and 1.2 % potassium (K), surpassing typical soil nutrient levels and exhibiting comparable NPK content to organic fertilizers. These results highlight the potential of EP-LWAs as an energy-efficient and eco-friendly planting materials, offering a cost-effective for sustainable agriculture, green roof, and vertical gardening applications.

1. Introduction

Climate change has become a major factor contributing to the reduction of green spaces, with rising temperatures, unpredictable weather patterns, and natural disasters accelerating the degradation of natural landscapes. Furthermore, rapid urbanization and increasing population density have led to the expansion of cities and the construction of high-rise buildings, infrastructure, and commercial spaces which further constrain access to outdoor areas. In response to these challenges, advancements in lightweight cementitious materials have played a pivotal role in supporting sustainable construction, particularly by enabling the creation of high-performance, low-density components suitable for urban greening systems. For instance, foam concrete technologies have been developed with improved rheological control, thermal insulation performance, and CO_2 sequestration capabilities, offering multifunctional benefits for environmental applications [1–3]. To mitigate the loss of green space and improve urban livability, innovative strategies have been developed to add greenery to residential spaces, such as vertical gardens and green roofs [4–6]. These green spaces improve air quality by filtering pollutants and releasing oxygen, while also reducing energy consumption through thermal insulation. Furthermore, the presence of green spaces supports mental health by reducing stress and promoting healthy urban lifestyle [7–9].

Porous ceramic pellets, also known as lightweight aggregate (LWA), have been recognized for their low density and high porosity [10], making them a promising planting material in modern greenery systems [11–13]. Their unique properties are advantageous in urban applications, as they significantly reduce the structural load on buildings, allowing green roofs and vertical gardens to be integrated without harming structural integrity. Additionally, LWA is highly effective at enhancing water retention and aeration [11–13], which are both critical factors for plant health. The porous nature of LWA allows it to absorb and store water efficiently, ensuring a consistent supply of moisture to plant roots.

Traditional LWAs are typically produced by firing naturally occurring expandable materials, such as clay, shale, and slate, at high temperatures [14–16]. This process results in a porous and lightweight aggregate that is highly suitable for various applications, including

* Corresponding author.
E-mail address: mettaya.ki@kmitl.ac.th (M. Kitiwan).

https://doi.org/10.1016/j.oceram.2025.100790
Received 13 March 2025; Received in revised form 23 April 2025; Accepted 25 April 2025
Available online 25 April 2025

construction and horticulture [14]. Although these natural materials are generally inexpensive, the firing temperature required for their production is considerably high, typically ranging between 1000 °C and 1300 °C [14,16]. This high-temperature process is energy-intensive, raising concerns about its sustainability in terms of energy consumption and carbon emissions. Moreover, the availability of natural expandable materials is often geographically constrained, posing challenges for widespread adoption in regions with limited resource availability.

Furthermore, growing concerns about resource depletion and environmental sustainability have driven research into alternative methods for fabricating LWAs from waste materials. Numerous studies have investigated the feasibility of incorporating industrial by-products and waste materials, such as fly ash, blast furnace slag, sewage sludge, recycled glass and plastics, and construction dust, into LWAs production [15–19]. These approaches not only offer a sustainable solution to waste management but also reduce the reliance on natural resources, promoting a circular economy and minimizing the environmental footprint of aggregate production.

In this research, expanded perlite (EP) waste, a by-product of construction industrial, was utilized as a secondary material to enhance the porous structure of LWAs produced from local red clay in Thailand. The red clay, commonly used in the production of pottery and bricks, was repurposed to create porous planting materials, offering an innovative and value-added application. The incorporation of EP not only facilitated the formation of internal pores within the pellets but also reduced the sintering temperature required for production. This is significant as the bloating process of conventional LWAs typically requires high temperatures [16], making this approach more energy-efficient and environmentally sustainable. The resulting porous LWAs offer great potential as effective planting materials for horticultural and agricultural applications.

However, a significant challenge with ordinary LWAs is that they often lack essential plant nutrients, which can limit their effectiveness in supporting plant growth. To overcome this limitation, researchers have investigated the incorporation of fertilizers into LWAs, resulting in a nutrient-rich planting medium that can provide a supply of vital nutrients for plants. Andreola et al. [20] examined the use of spent coffee grounds (SCGs) and tailored fertilizer glass (FG) in producing LWAs. The SCGs were used as a pore-forming agent, while the FG, made with cattle bone flour ash (CBA) and potassium carbonate, provided P and K nutrients. The LWAs demonstrated high porosity (43.6–55.5 %), high water absorption (15.9 – 46.8 %) low bulk density (1.12–1.42 g/cm^3), and controlled nutrient release (87.7 % P and 25.7 % K over 21 days). Martinez-Garcia et al. [21] reported the production of LWAs using clays blended with brewery wastewater sludge as a pore-forming agent, cattle bone flour ash (CBA), and fertilizer glass (FG) to incorporate K and P as plant nutrients. The LWAs were sintered at 1000 °C, achieving porosity values up to 54.78 %, pH levels ranging from 6.5 to 7.5, and electrical conductivity (E.C.) values below 2 mS/cm, making them suitable for agricultural applications. Nutrient leaching tests revealed that FG-based LWAs provided a controlled release of K and P over time. Barbi et al. [22] investigated the development of LWAs coated with nitrogen-enriched biomass from black soldier fly (BSF). LWAs were prepared using red clay, PK-enriched fertilizer glass and bone flour ash, then they were coated with a glycerol-based mixture. The results showed controlled release of NPK over 21 days. Ronga et al. [23] studied the development of LWAs using red clay, spent coffee grounds (SCGs), biochar, and tailored fertilizer glass (FG) composed of cattle bone flour ash, potassium carbonate, and packaging glassy sand. The materials were processed into LWAs via powder sintering at 1000 °C, achieving high porosity (42–45 %), pH suitability (6.5–8.3), and nutrient release properties, including P and K availability over 90 days. According to these studies, most research utilized complex processes, such as multi-step coating techniques, advanced material formulations, or the use of specialized additives, which may become limitations for large-scale industrial applications. Therefore, developing simpler and more efficient approaches for integrating plant nutrients into LWA is necessary for overcoming current challenges and facilitating their practical implementation on an industrial scale.

This study aims to develop LWAs incorporated with NPK fertilizer for use as a nutrient-enriched planting material. The research is divided into two main parts. The first part focuses on the preparation of the integration of EP into LWAs with EP content ranging from 0 to 40 wt. % and examines the sintering conditions of EP-LWAs at temperatures between 800 °C and 1000 °C. The objective is to achieve optimal physical properties, including bulk density, porosity, and water absorption, while minimizing energy consumption through lower-temperature sintering. The second part of the study aims to enhance the functionality of EP-LWAs as a nutrient-enriched planting material by incorporating NPK fertilizer. A simple vacuum infiltration technique is employed to ensure efficient nutrient loading and retention within the porous structure. This modification attempts to promote the efficient use of LWAs in horticulture. The outcomes of this study contribute to the advancement of innovative, resource-efficient growing media, aligning with sustainable agriculture and circular economy principles.

2. Materials and methods

2.1. Raw materials and LWAs preparation process

In this study, raw red clay (sourced locally from Phan Thong, Chonburi, Thailand) and expanded perlite (EP) waste (from Klong Yang Co., Ltd. Thailand) were used as the main raw materials. The EP waste used in this study is primarily used as an additive in cement-based wall coatings for thermal insulation. The waste material consisted of fine particles that did not meet the commercial size specifications, typically removed during production through an air-blowing separation process. Carboxyl methyl cellulose (CMC; Chemipan Corporation Co., Ltd., Thailand) was prepared in a 0.05 wt % solution for use as a binder in the preparation of raw clay pellets. A low concentration of CMC (0.05 wt. %) was incorporated to enhance plasticity and cohesion during pelletizing, without significantly affecting the final porosity or other physical properties of the EP-LWAs. To ensure consistency and reliability across experimental batches, each batch of main raw materials was characterized prior to use. The chemical compositions of the red clay and expanded perlite were analyzed using X-ray fluorescence spectroscopy (XRF; Rigaku, ZSX Primus IV, Japan). In addition, the crystalline phases of raw materials were characterized using X-ray diffraction (XRD; Miniflex 600, Rigaku, Japan) with Cu Kα radiation over a 2θ range of 10–80° with a scanning speed of 0.02° min^{-1}.

The LWAs were produced by partially replacing red clay with EP at varying proportions ranging from 0 to 40 wt.%. Firstly, the red clay was pulverized and sieved through a 200-mesh (74 μm) sieve, while the EP was separately sieved using the same mesh size. Subsequently, the red clay powder and EP were then dry mixed in the mixer machine. After mixing for 5 min, the CMC solution was gradually added to the mixer machine and further mixed for 10 min to ensure uniformity and enhance workability. The clay mixture with appropriate plasticity was transferred to a pelletizing machine to form spherical pellets with a diameter of approximately 8 mm. The pellets were subsequently dried in an oven at 105 °C for 24 h. The dried pellets were placed in alumina crucibles and sintered in an electric furnace at temperatures of 800 °C, 900 °C, and 1000 °C for 2 h.

2.2. Physical properties characterization

After sintering, the physical properties, including bulk density, porosity, and water absorption, of the porous ceramic pellets were evaluated in compliance with the ASTM C20 standard [24]. Initially, the porous ceramic pellets were immersed in deionized (DI) water and boiled for 6 h to remove air from within the pores. After that, the pellets

were cooled to room temperature and left immersed in DI water for at least 12 h. The pellets were then weighed in DI water to determine the suspended weight (S) and subsequently weighed in the air to determine the saturated weight (W). Following this, the pellets were dried in an oven at 120 °C for 24 h and weighed again to obtain the dry weight (D). The volume (V) of the pellets was calculated by subtracting the suspended weight from the saturated weight, i.e., $V = W - S$. Using these measurements, the bulk density, porosity, and water absorption of the LWAs were calculated using the following equation:

$$\text{Bulk Density} = \frac{D}{V} \quad (1)$$

$$\text{Porosity} = \frac{W-D}{V} \times 100\% \quad (2)$$

$$\text{Water absorption} = \frac{W-D}{V} \quad (3)$$

2.3. Fertilizer incorporation process

To prepare the NPK-incorporated LWAs, a 0.15 wt% CMC solution was used as an absorbing medium for fertilizer incorporation. A compound fertilizer, NPK 16–16–16 (Chai Tai, Thailand), was utilized as the nutrient source. For the fertilizer incorporation step, a higher CMC concentration (0.15 wt.%) was selected because of its role as an absorbing and retaining medium. Preliminary testing showed that concentrations above 0.15 wt.% led to poor homogeneity and particle aggregation, which hindered uniform fertilizer distribution. The fertilizer incorporation process is depicted in Fig. 1. The compound fertilizer granules were ground into fine powder using a mortar and pestle. For the preparation of the fertilizer solution, 30 g, 40 g, and 50 g of ground fertilizer were dissolved in 100 mL of CMC solution to achieve three different concentrations. The mixture was stirred using a magnetic stirrer for 30 min to ensure thorough blending, resulting in the NPK/CMC solution.

Approximately 30 sintered EP-LWA pellets (total weight ~10 g) were immersed in the prepared NPK/CMC solution and placed in a vacuum desiccator (internal volume ~9 L) connected to a two-stage rotary vane vacuum pump (VALUE VRI-4, Value Vacuum Technology, China; ultimate pressure 2×10^{-1} Pa, flow rate 4.0 m^3/h). The system was evacuated to a gauge pressure of −760 mmHg (approx. 1.3 kPa) and maintained for 3 h to facilitate infiltration. These conditions were selected based on preliminary trials to ensure complete absorption of the NPK/CMC solution into the internal pores without inducing structural damage. The infiltration was considered complete when no air bubbles were observed escaping from the pellet surfaces. The 3-hour duration was found to be optimal, as shorter times led to incomplete infiltration, while longer durations did not result in further solution uptake. After that, the pellets were removed from the vacuum desiccator, an excess solution was filtered out, and they were dried in an oven at 70 °C for 24 h. The prepared samples were designated as EP-LWA-F30, EP-LWA-F40, and EP-LWA-F50, corresponding to the respective weight percentages of fertilizer used in the preparation.

For the analysis of NPK-embedded LWAs microstructure, a Scanning Electron Microscope (SEM; FEI, Quanta 250, USA) was used coupled with an Energy Dispersive X-Ray Spectrometer (EDS; Oxford Instruments, UK).

2.4. Analysis of chemical fertilizer in LWAs

The fertilizer content in the NPK-incorporated LWAs was analyzed according to the Notification of the Ministry of Agriculture and Cooperatives of Thailand; *Re.* Prescribing the Method of Analysis of Chemical fertilizers B.E. 2559 [25], which prescribes the methods for chemical fertilizer analysis. The test methods and corresponding standard numbers for each fertilizer component are as follows:

- Total Nitrogen (TN): Combustion method (Method 1.05.02).
- Total Phosphorus (TP_2O_5): Spectrophotometric Molybdovanadophosphate Method (Method 1.09.01).
- Water Soluble Potassium (WK_2O): Inductive Couples Plasma Emission Spectroscopic method (Method 1.12.01).

3. Results and discussion

3.1. Chemical composition and phase analysis of raw materials

The chemical compositions of red clay and expanded perlite analyzed by XRF are presented in Table 1. The results indicate that red clay primarily consists of 66.9 % SiO_2, along with notable proportions of Al_2O_3 (22.3 %) and Fe_2O_3 (4.85 %), which contribute to its refractory nature and structural stability. These elements are commonly found in various soil types and play a crucial role in the sintering process by enhancing thermal stability and densification. Expanded perlite, exhibits a higher SiO_2 content (75.4 %) compared to red clay, along with minor content of Al_2O_3 (13.6 %) and Fe_2O_3 (1.33 %). This variation in composition is due to its natural formation as a volcanic glassy mineral, where the high silica content enhances its thermal expansion and bloating behavior when heated, making it an ideal component for LWA. Additionally, expanded perlite contains higher Na_2O (1.59 %) and K_2O (6.75 %), which could act as fluxing agents during sintering, facilitating the formation of an interconnected porous structure.

The XRD results of phases for raw material analysis are presented in Fig. 2. In the red clay phase, as shown in Fig. 2(a), quartz (SiO_2) is identified as the dominant crystalline phase, evidenced by the strong peak at 26.6°. This is consistent with the XRF data, which showed high SiO_2 content in the red clay. Additionally, kaolinite ($Al_2Si_2O_5(OH)_4$) and illite ($KAl_2(Si_3Al)O_{10}(OH)_2$) are identified as major clay minerals, contributing to the plasticity and binding properties of the clay. The presence of hematite (Fe_2O_3) is confirmed by peaks in the 33–35° range, which account for the red coloration of the clay due to iron oxides. Furthermore, feldspar (orthoclase, $KAlSi_3O_8$) is detected at diffraction peaks around 27–29°, where it can act as fluxing agent during sintering process. The combination of quartz, kaolinite, illite, hematite, and

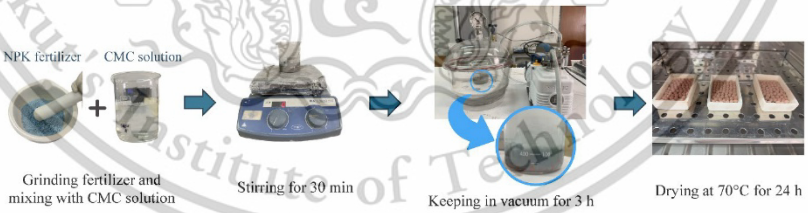

Fig. 1. Schematic diagram of the fertilizer incorporation processes in LWAs.

Table 1
The oxide chemical compositions of red clay and expanded perlite.

Component (wt%)	SiO_2	Al_2O_3	Fe_2O_3	K_2O	TiO_2	MgO	Na_2O	Na_2O	CaO	P_2O_5
Red clay	66.9	22.3	4.85	1.92	1.01	0.60	0.30	0.30	0.21	0.06
Expanded perlite	75.4	13.6	1.33	6.75	0.29	0.20	1.59	1.59	0.69	0.01

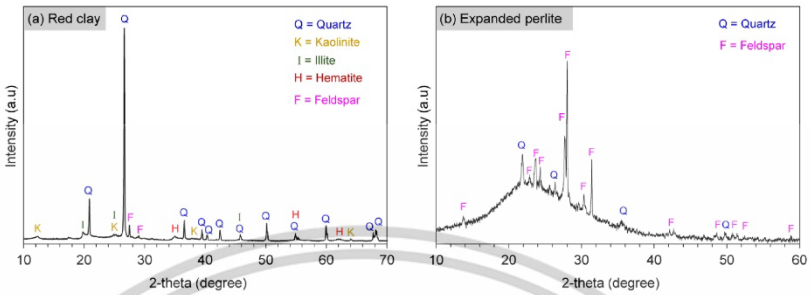

Fig. 2. XRD patterns of phases identification in the raw materials: (a) red clay and (b) expanded perlite.

feldspar makes this red clay an excellent candidate for LWA production.

The XRD pattern of expanded perlite, as illustrated in Fig. 2(b), exhibits a broad peak between 15° and 35°, indicating a dominant amorphous phase. This suggests that expanded perlite is primarily composed of a non-crystalline silicate matrix, which is due to its formation through rapid cooling of volcanic glass. Additionally, small diffraction peaks in the XRD pattern suggest the presence of minor crystalline phases, likely including quartz (SiO_2) and feldspar (orthoclase, $KAlSi_3O_8$). These compositions characteristic support the suitability of expanded perlite in enhancing porosity in LWAs.

3.2. Physical properties of LWAs after sintering

Fig. 3 illustrates the color transformation of EP-LWAs (20 wt.% EP) before and after sintering at different temperatures. The raw clay pellets exhibit a dark brown color, which progressively changes to light orange at 800 °C and becomes more pronounced as the sintering temperature increases. At 1000 °C, the pellets develop a deeper reddish-orange shade, indicative of phase changes occurring within the material. This color change is primarily due to the iron (Fe) component in the raw clay, which oxidizes during the sintering process. The formation of hematite (Fe_2O_3), a common iron oxide responsible for red and orange hues in fired ceramics, is the key to this transformation. As the temperature

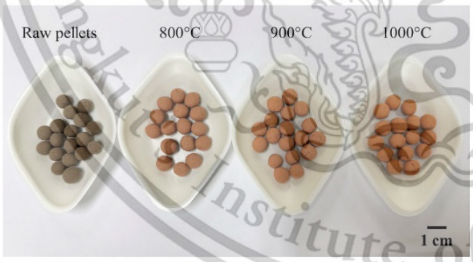

Fig. 3. The color transformation of EP-LWAs (20 wt.% EP) before and after sintering at 800 °C, 900 °C, and 1000 °C.

increases, the oxidation of Fe^{2-} to Fe^{3-} becomes more pronounced, leading to an intensified orange-red coloration. This phenomenon is widely observed in iron-rich clays, where the interaction between iron and oxygen at elevated temperatures facilitates the development of hematite crystalline phases [26].

The average diameter of the raw pellets was approximately 7.86 mm. After sintering at 800 °C, the diameter of all samples showed a slight expansion, ranging from 1.45 % to 2.74 %. This behavior is primarily attributed to transformations within the red clay matrix, such as the dehydroxylation of kaolinite ($Al_2Si_2O_5(OH)_4 \rightarrow Al_2Si_2O_7 + H_2O$) [27], the release of structural water, and the decomposition of residual organic matter and carbonates, which may result in localized pore formation and limited swelling. However, as the temperature increased to 900 °C and 1000 °C, the pellets exhibited progressive shrinkage, with diameter reductions ranging from 0.25 % to 0.97 % at 900 °C and 0.25 % to 9.46 % at 1000 °C. This shrinkage indicates a shift toward densification mechanisms, including particle coalescence and viscous flow sintering. Notably, the EP, which had already undergone thermal expansion during its original production, did not contribute to further bloating at these temperatures. Instead, it likely softened and collapsed under high thermal stress, contributing to overall volume reduction. Furthermore, the formation of a glassy phase from feldspar or silica components in the clay matrix likely enhanced sintering, resulting in a net shrinkage of the pellets.

Fig. 4 displays the XRD patterns of EP-LWAs containing 20 wt.% EP, sintered at 800 °C, 900 °C, and 1000 °C. Quartz remains the dominant crystalline phase, as indicated by the consistent and intense peak at $2\theta \approx 26.6°$. Feldspar peaks, notably around 27.8°–28.0°, are also present and increase slightly with increasing sintering temperature, suggesting recrystallization from the molten glassy phase upon cooling. In contrast, peaks of kaolinite and illite observed in the raw clay are no longer detectable after sintering, particularly above 900 °C. This disappearance indicates the thermal dehydroxylation and phase transformation of these clay minerals. Specifically, kaolinite begins to transform into metakaolinite around 400–500 °C and may further convert into spinel-type or mullite precursors at temperatures exceeding 900 °C [28]. However, diffraction peaks corresponding to mullite or other crystalline aluminosilicates are not observed, likely due to their low concentration or the formation of poor crystalline phases. Hematite peaks are also not clearly discernible, possibly due to their minor presence or overlap with

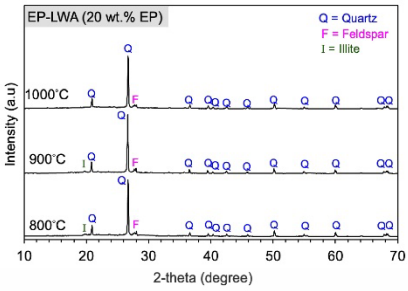

Fig. 4. XRD patterns of EP-LWAs containing 20 wt.% EP, sintered at 800 °C, 900 °C, and 1000 °C.

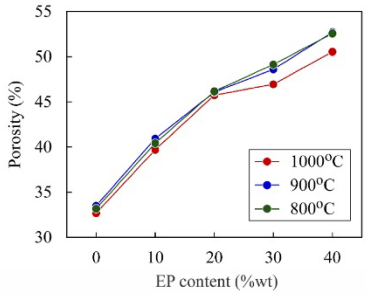

Fig. 6. Effect of expanded perlite (EP) content on the porosity of EP-LWAs sintered at 800 °C, 900 °C, and 1000 °C.

other phases. These XRD analysis confirms phase changes during sintering, characterized by the decomposition of unstable clay minerals and the persistence of quartz and feldspar, indicating a transition toward a more vitrified and thermally stable microstructure. It is noteworthy that EP-LWAs with other EP contents exhibited similar XRD patterns, suggesting consistent phase evolution across different compositions.

The relationship between expanded perlite content and bulk density of EP-LWAs sintered at different temperatures is shown in Fig. 5. The results indicate a progressive decrease in bulk density with increasing EP content, regardless of the sintering temperature. At 0 wt.% EP, the bulk density is the highest (~1.8 g/cm^3) due to the compact nature of the clay matrix. As the EP content increases, the bulk density decreases steadily, reaching ~0.9 g/cm^3 at 40 wt.% EP. This trend is attributed to the low intrinsic density and porous structure of EP, which reduces the overall material compactness when incorporated into the LWAs formulation. Additionally, the effect of sintering temperature on bulk density is observed. At higher temperatures (1000 °C), the bulk density is slightly higher than at 900 °C and 800 °C, suggesting enhanced densification and sintering at elevated temperatures. The slight compaction at 1000 °C could be due to the partial softening and collapse of amorphous silica in EP, leading to increased material consolidation. However, despite this effect, the overall bulk density still follows a downward trend with increasing EP content. These results confirm that EP effectively reduces the density of LWAs, making them suitable for lightweight applications, particularly in horticulture and green roofing.

The effect of expanded perlite content on the porosity of EP-LWAs is illustrated in Fig. 6. The results demonstrate a positive correlation between EP content and porosity, where increasing the EP content leads to an increase in porosity across all sintering temperatures. At 0 wt.% EP, the porosity is the lowest (~33–34 %), as the clay matrix is relatively dense. When the EP content increases, the porosity rises steadily, reaching ~50–53 % at 40 wt.% EP. This trend is attributed to the intrinsically porous nature of EP, which contributes additional void spaces within the ceramic matrix, thereby increasing overall porosity of LWAs. The influence of sintering temperatures is also evident. While all temperatures exhibit similar trends, porosity is slightly lower at 1000 °C compared to 900 °C and 800 °C. This slight reduction is likely due to partial softening and densification of EP particles at high temperatures, causing some pore collapse and reducing porosity. Conversely, at lower sintering temperatures (800 °C and 900 °C), EP maintains its structure, resulting in higher porosity retention.

The increase in bulk density and slight reduction in porosity observed at 1000 °C can be attributed to enhanced densification mechanisms characteristic of ceramic sintering. At this temperature, partial vitrification occurs as feldspar and silica phases in the red clay and EP begin to soften, promoting viscous flow, neck formation, and grain boundary diffusion, which facilitate a slight shrinkage of the pore. In this study, the EP having previously undergone industrial bloating, does not re-expand but instead softens and collapses under heat, further contributing to reduced open porosity. While densification improves the mechanical strength of the EP-LWAs, it may slightly reduce their water retention capacity, which is a critical factor for horticultural applications. Therefore, there is a trade-off between mechanical robustness and functional porosity.

The relationship between expanded perlite content and water

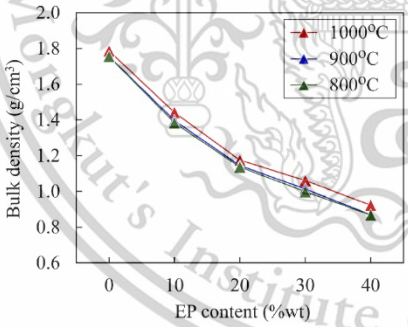

Fig. 5. Effect of expanded perlite (EP) content on the bulk density of EP-LWAs sintered at 800 °C, 900 °C, and 1000 °C.

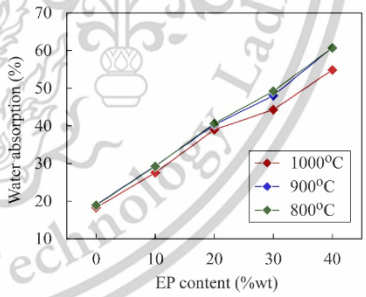

Fig. 7. Effect of expanded perlite (EP) content on the water absorption of EP-LWAs sintered at 800 °C, 900 °C, and 1000 °C.

absorption of EP-LWAs is illustrated in Fig. 7. The results show a linear increase in water absorption with increasing EP content, indicating that the incorporation of EP significantly enhances the water-holding capacity of LWAs. At 0 wt.% EP, the water absorption is the lowest (~18–19 %), as the clay matrix is denser and less porous. As the EP content increases, water absorption rises steadily, reaching ~55–61 % at 40 wt. % EP. This trend is attributed to the intrinsically porous nature of EP, which introduces additional void spaces into the LWAs structure, thereby increasing its ability to retain water. The effect of sintering temperature is also observed, with higher temperatures (1000 °C) leading to slightly lower water absorption compared to 900 °C and 800 °C. This reduction can be explained by increased densification and partial collapse of pores at higher sintering temperatures, which limits the number of interconnected voids available for water retention. However, despite this effect, the overall trend remains consistent, with higher EP consistently leading to greater water absorption across all sintering temperatures.

The selection of optimal sintering conditions and EP content for the further NPK incorporation process must consider suitable porosity, mechanical strength, and energy consumption. High porosity is essential for efficient fertilizer absorption and retention, while adequate mechanical strength ensures that the LWAs remain intact during handling and application. Additionally, minimizing energy consumption is crucial for ensuring the sustainability of the production process. The findings indicate that increasing EP content enhances porosity and water absorption, making the LWAs more suitable for fertilizer loading. However, excessively high EP content, 30–40 wt. %, results in mitigates mechanical strength, causing the pellets more fragile. Conversely, 20 wt. % EP provides an optimal balance between porosity and structural integrity, ensuring sufficient nutrient absorption while maintaining durability.

Sintering temperature also plays a crucial role in determining the final properties of the pellets. At 800 °C, the LWAs exhibit the highest porosity and water absorption, but their mechanical strength is likely insufficient due to limited densification. Additionally, while 1000 °C improves mechanical strength through increased densification, it also reduces porosity and water absorption, limiting its effectiveness for fertilizer incorporation. Moreover, the higher energy consumption associated with 1000 °C sintering makes it less sustainable. In this research, the most suitable sintering temperature is 900 °C, which provides moderate porosity, improved structural stability, and balanced energy efficiency. It is well-known that reducing the sintering temperature from conventional ranges of 1000–1300 °C to as low as 900 °C, as optimal temperature in this study, can contribute substantially to lowering thermal energy input and associated carbon emissions. The ability to produce porous EP-LWAs with favorable physical properties at a lower processing temperature supports a more energy-efficient and sustainable manufacturing route. Additionally, the use of waste-derived expanded perlite as a pore-forming material further enhances the environmental profile of the process by promoting waste valorization and reducing reliance on costly raw materials. Therefore, for the next stage of NPK incorporation, LWA with 20 wt.% EP sintered at 900 °C is selected as the most appropriate one. Under this sintering condition, the EP-LWA exhibited a bulk density of 1.2 g/cm^3, a porosity of 46.1 %, and a water absorption of 40.3 %.

The physical properties of the optimized EP-LWAs developed in this study were compared with three commercially available LWAs commonly used in horticultural applications, as shown in Table 2. The EP-LWAs exhibited a slightly smaller average diameter (8.16 mm) than the commercial products (9.02–9.31 mm), indicating their suitability for applications requiring finer aggregate sizes. In terms of bulk density, the EP-LWAs demonstrated significantly higher values (1.15 g/cm^3) compared to the commercial samples (0.56–0.68 g/cm^3). This higher density suggests improved mechanical robustness, which may be advantageous for structural integrity in green roof or vertical garden applications. Although the EP-LWAs showed slightly lower porosity (46.1 %) and water absorption (40.3 %) than some commercial products (porosity up to 53.0 %, water absorption up to 94.9 %), their values still fall within a practical range for horticultural use. The moderate water absorption capacity ensures adequate moisture retention while avoiding excessive water retention that could lead to root rot [29]. This balance is particularly advantageous in controlled irrigation systems, where substrate water management is critical for plant health and productivity.

Table 2
Comparison of physical properties between EP-LWAs developed in this study and commercially available LWAs used in horticulture.

Samples	Average diameter (mm)	Bulk density (g/cm^3)	Porosity (%)	Water absorption (%)
Commercial LWA no.1	9.31	0.56	53.0	94.9
Commercial LWA no.2	9.25	0.68	43.8	64.6
Commercial LWA no.3	9.02	0.56	49.5	88.1
EP-LWA (20 wt %EP) (This study)	8.16	1.15	46.1	40.3

3.3. Analysis of fertilizer in NPK-incorporated LWAs

After the NPK incorporation process in LWAs, the 50 wt.% fertilizer-loaded sample was selected for elemental analysis to assess nutrient distribution. The cross-section of the NPK-incorporated LWAs, along with the corresponding EDS elemental mapping for key elements in the clay region and EP region, is presented in Figs. 8 and Fig. 9, respectively. The quantitative analysis of elemental composition of each region is summarized in Table 3.

The main elements in LWA are O, Si, and Al, primarily due to the presence of silicates, aluminosilicates, and oxides in the ceramic matrix. Si content slightly higher in the EP region (25.14 %) than in the clay region (21.61 %), which aligns with its natural composition as a volcanic glass material. The elevated C content detected in both regions (9.51 % in EP and 11.61 % in clay) is attributed to CMC, a carbon-rich polymer, which was used as an absorbing medium for the NPK incorporation process. Fe is more concentrated in the clay region (2.44 %) than in the EP region (1.44 %), confirming that iron-rich phases are more dominant in the natural clay matrix.

The key components of fertilizer, K and P, are detected in both regions, confirming fertilizer incorporation within the porous LWAs. The content of K is higher in the EP region (3.33 %) than in the clay region (2.12 %), suggesting better nutrient retention in perlite-dominant areas. The concentration of P is slightly higher in the clay region (0.79 %) than in the EP region (0.27 %), indicating that the clay phase plays a role in P adsorption and retention. EP possesses a highly porous, glassy silicate structure with a large, interconnected pore network that may facilitate greater physical entrapment of soluble nutrients, particularly K, which is more mobile and easily diffused. Previous research reported that EP demonstrated remarkable nutrient adsorption capacity, exceeding ion exchange expectations and suggesting the involvement of physisorption mechanisms [30]. Their experiments confirmed that perlite can retain nutrients through physisorption mechanisms, increasing nutrient residence time in soil systems [30]. In contrast, clay minerals, especially those rich in Fe and Al, have high affinities for phosphate ions [31]. Moreover, P ions are generally less mobile and are readily adsorbed or fixed by clay minerals, particularly through chemical binding with Fe and Al oxides and hydroxyl groups on clay surfaces [31].

The EDS results confirm the successful incorporation of NPK fertilizer elements (K and P) into the porous LWA, with noticeable distribution across both the clay and EP regions. Unfortunately, nitrogen (N), another key fertilizer element, was not detected by EDS due to its low

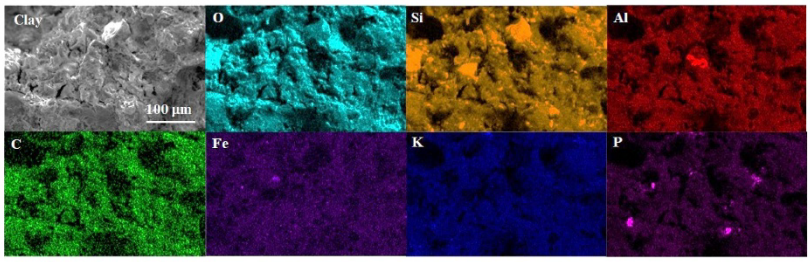

Fig. 8. SEM image of the cross-section of NPK-incorporated LWA in clay region with EDS mapping showing composition and distribution of key elements.

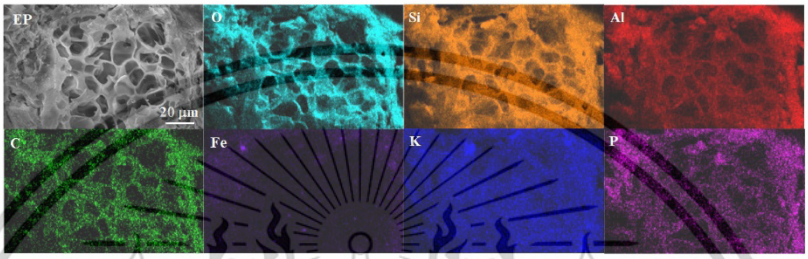

Fig. 9. SEM image of the cross-section of NPK- incorporated LWA in EP region with EDS mapping showing composition and distribution of key elements.

Table 3
The EDS analysis of each element in NPK-incorporated LWA.

Elements (wt%)	O	Si	Al	C	Fe	K	P
Clay	46.21	21.61	7.36	11.61	2.44	2.12	0.79
EP	46.16	25.14	6.64	9.51	1.44	3.33	0.27

atomic number and weak interaction with X-rays, which makes it challenging to identify using standard EDS detection methods.

The nutrient content in NPK-incorporated EP-LWAs was also analyzed following the Thai Standard Method for Chemical Fertilizer Analysis [25] to determine the levels of total nitrogen (TN), total phosphorus (TP_2O_5), and water-soluble potassium (WK_2O). The results, as shown in Table 3, demonstrate the effectiveness of the EP-LWAs in retaining essential nutrients for potential horticultural applications. The nutrient analysis reveals a progressive increase in TN, TP_2O_5, and WK_2O content as the fertilizer loading in EP-LWA increases. EP-LWA-F30 shows 1.3 % N, 1.1 % P, and 1.4 % K. EP-LWA-F40 contains 1.9 % N, 1.5 % P, and 2.1 % K, whereas EP-LWA-F50 exhibits the highest nutrient content, with 2.2 % N, 1.8 % P, and 2.9 % K. This trend indicates that higher fertilizer loading enhances the overall nutrient retention within the porous structure of the LWAs. Among the macronutrients analyzed, K exhibits the highest concentration, suggesting that water-soluble potassium is effectively retained within the LWAs and readily available for plant uptake. The P content also increases with higher fertilizer incorporation, indicating the potential for sustained phosphorus release. Meanwhile, the N levels are relatively moderate, likely due to nitrogen having higher mobility and susceptibility to volatilization during preparation process.

Soil fertility is commonly assessed using key macronutrient parameters, including total nitrogen (N), extractable phosphorus (P), and extractable potassium (K). According to the Thai soil fertility classification system [32], N content is categorized as low (<0.1 %), medium (0.1–0.2 %), and high (>0.2 %). Similarly, P_2 is classified as low (<10 mg/kg), medium (10–25 mg/kg), and high (>25 mg/kg). K follows a similar classification, where low fertility soils contain <60 mg/kg, medium 60–90 mg/kg, and high fertility soils >90 mg/kg. These classifications serve as general indicators of soil nutrient availability for plant growth and are widely used in agricultural and environmental assessments.

When comparing the nutrient content of EP-LWAs with Thai soil fertility ratings, it is evident that NPK-incorporated EP-LWAs exhibit significantly higher nutrient concentrations than naturally occurring high-fertility soils. For instance, the N content in EP-LWAs (1.3–2.2 %) exceeds the high-fertility threshold (>0.2 %), indicating that EP-LWAs serve as a rich nitrogen source for plant nutrition. Similarly, P content in EP-LWAs ranges from 1.1 % to 1.8 % (equivalent to 11,000–18,000 mg/kg) which is superior to the high-fertility soil threshold of 25 mg/kg. This significant difference highlights that EP-LWAs serve as an exceptionally rich phosphorus source. K levels in EP-LWAs, ranging from 1.4 % to 2.9 % (equivalent to 14,000–29,000 mg/kg), are drastically higher than the high-fertility soil threshold (>90 mg/kg), suggesting that EP-LWAs can act as an excellent K source.

According to the Thai Agricultural Commodity and Food Standards (TAS 9503–2005) for compost [33], organic fertilizers must meet specific nutrient criteria to ensure their effectiveness in supporting plant growth. The standard defines primary nutrients such as total nitrogen (N), total phosphorus (P_2O_5), and total potassium (K_2O) with minimum required concentrations of ≥ 1.0 % N, ≥ 0.5 % P_2O_5, and ≥ 0.5 % K_2O by weight. When compared with the nutrient content of NPK-incorporated EP-LWAs, the results indicate that EP-LWAs exceed the Thai compost standards in all nutrient categories. For example, the N in EP-LWAs ranges from 1.3 % to 2.2 %, which is well above the 1.0 % minimum set by TAS. Similarly, P in EP-LWAs (1.1 %–1.7 %) is significantly greater than the 0.5 % requirement, confirming its high phosphorus

retention capability. Furthermore, K in EP-LWAs (1.4 %–2.9 %) is more than double the 0.5 % K_2O threshold, indicating excellent potassium availability for plant uptake.

The nutrient content of NPK-embedded EP-LWAs was compared with commonly used organic fertilizers, including cow manure, pig manure, rice straw, and cassava stem (Table 4). The results indicate that EP-LWAs contain significantly higher concentrations of essential nutrients, NPK, than most organic fertilizers. Compared to conventional organic fertilizers, EP-LWAs provide a higher and more balanced NPK content, particularly in P and K which are often limiting nutrients in soil. This makes EP-LWAs a promising alternative or complementary material for soil amendment in sustainable agriculture and urban gardening.

It is important to note that the NPK contents reported in this study were obtained through static chemical analysis based on the Thai Agricultural Standard [25], which measures the total amount of NPK fixed within the EP-LWA samples. These values reflect the nutrient loading capacity but do not provide information about the release behavior over time. To fully evaluate the potential of EP-LWAs as nutrient carriers for horticultural applications, future work will focus on investigating the release kinetics of N, P, and K using standard leaching tests which thereby offering deeper insight into their functional performance as planting substrates.

In this study, the vacuum infiltration method was selected for its simplicity, reproducibility, and ability to achieve deep nutrient penetration into the porous EP-LWAs without requiring complex equipment or chemical modification. While this approach is effective at the laboratory scale, further work is needed to assess its scalability. Alternative methods such as surface coating or spraying may offer higher throughput, but tend to localize nutrients on the surface, increasing leaching risk. A hybrid strategy that combines simplified vacuum soaking with surface application may provide a promising pathway for future large-scale production.

In addition to their lightweight nature and nutrient retention capability, EP-LWAs offer several functional benefits for green roof and vertical garden applications. Their high porosity promotes root aeration and water retention, supporting plant health in space-limited environments. The porous ceramic structure also contributes to thermal insulation, helping to moderate root zone temperatures and reduce heat stress. Moreover, EP-LWAs are dimensionally stable and non-degradable, providing long-term durability compared to organic media such as peat.

These findings highlight the potential of NPK-incorporated EP-LWAs as nutrient-enriched planting materials, particularly for green roof and vertical garden applications. The porous structure of EP-LWAs not only enhances nutrient retention, but also supports lightweight, well-aerated substrates suitable for urban greening systems. EP-LWAs can improve plant growth efficiency in space-limited environments, making them an eco-friendly alternative to typical soil in urban agriculture and sustainable landscape designs.

4. Conclusion

This study successfully developed and characterized expanded perlite-lightweight aggregates (EP-LWAs) incorporated with NPK fertilizer, demonstrating their potential application in sustainable agricultural and horticultural application. The optimization of sintering conditions revealed that 900 °C was the most suitable temperature for fabricating EP-LWAs with suitable physical properties, i.e. a bulk density of 1.15 g/cm^3, porosity of 46.09 %, and water absorption of 40.28 %. These properties ensure lightweight characteristics and effective nutrient retention, making EP-LWAs suitable for use in green roofs, vertical gardens, and soil amendment applications. The nutrient analysis confirmed that EP-LWAs with 50 g fertilizer loading contained 2.2 % N, 1.8 % P, and 2.9 % K, which exceeds typical NPK levels found in Thai soils and surpasses the minimum requirements set by compost fertilizer regulations. These findings highlight EP-LWAs as a superior nutrient carrier, offering a balanced and enriched nutrient profile compared to conventional organic fertilizers such as manure and agricultural residues. Furthermore, the integration of fertilizer into the porous EP-LWA matrix suggests enhanced nutrient retention, potentially reducing nutrient leaching losses while ensuring prolonged nutrient availability for plant uptake. However, future research should focus on detailed investigations of nutrient release kinetics, evaluating long-term performance in various soil conditions and plant growth studies to optimize their efficacy as slow-release fertilizers.

Table 4
Comparison of NPK nutrients in EP-LWAs with the NPK content in various types of organic fertilizers.

Samples		Nutrients		
		N (%)	P (%)	K (%)
This study	EP-LWA-F30	1.3	1.1	1.4
	EP-LWA-F40	1.9	1.5	2.1
	EP-LWA-F50	2.2	1.8	2.9
Organic fertilizers [32]	Cow manure	1.1	0.40	1.60
	Pig manure	1.3	2.40	1.00
	Rice straw	0.59	0.08	0.26
	Cassava stem	1.23	0.24	1.23

CRediT authorship contribution statement

Panadda Rungrueng: Writing – original draft, Visualization, Investigation, Formal analysis. **Montree Hankoy:** Visualization, Formal analysis, Data curation. **Mettaya Kitiwan:** Writing – review & editing, Validation, Supervision, Project administration, Methodology, Funding acquisition, Conceptualization. **Nittaya Keawprak:** Resources, Conceptualization. **Phacharaphon Tunthawiroon:** Writing – review & editing, Validation, Methodology, Conceptualization.

Declaration of competing interest

The authors declare the following financial interests/personal relationships which may be considered as potential competing interests: Mettaya Kitiwan reports financial support was provided by National Science, Research and Innovation Fund (NSRF). Panadda Rungrueng reports financial support was provided by King Mongkut's Institute of Technology Ladkrabang. If there are other authors, they declare that they have no known competing financial interests or personal relationships that could have appeared to influence the work reported in this paper.

Acknowledgments

This work by King Mongkut's Institute of Technology Ladkrabang (KMITL) was supported by National Science, Research and Innovation Fund (NSRF) under grant number RE-KRIS/FF65/19. This work is also supported by King Mongkut's Institute of Technology Ladkrabang [grant no. KREF016508], as *M.Sc.* scholarship for Panadda Rungrueng.

References

[1] D. Fan, J.X. Lu, X. Sen Lv, T. Noguchi, R. Yu, C.S. Poon, Carbon capture and storage CO_2 foam concrete towards higher performance: design, preparation and characteristics, Cem. Concr. Compos. 157 (2025) 105925, https://doi.org/10.1016/J.CEMCONCOMP.2025.105925.

[2] D. Fan, C. Zhang, J.X. Lu, L. Peng, R. Yu, C.S. Poon, Rheology dependent pore structure optimization of high-performance foam concrete, Cem. Concr. Res. 188 (2025) 107737, https://doi.org/10.1016/J.CEMCONRES.2024.107737.

[3] D. Fan, C. Zhang, X. Li, X. Lv, J.X. Lu, R. Yu, T. Noguchi, C.S. Poon, Development of Foam Concrete toward High Strength and CO_2 Sequestration, ACS Sustain. Chem. Eng. 12 (2024) 16622–16637, https://doi.org/10.1021/ACSSUSCHEMENG.4C05136/SUPPL_FILE/SC4C05136_SI_001.PDF.

[4] K. Al-Kodmany, Greenery-covered tall buildings: a review, Buildings 13 (2023) 2362, https://doi.org/10.3390/BUILDINGS13092362.

[5] J. Aleksejeva, G. Voulgaris, A. Gasparatos, Systematic review of the climatic and non-climatic benefits of green roofs in urban areas, Urban Clim 58 (2024) 102133, https://doi.org/10.1016/J.UCLIM.2024.102133.

[6] G. Mihalakakou, M. Souliotis, M. Papadaki, P. Menounou, P. Dimopoulos, D. Kolokotsa, J.A. Paravantis, A. Tsangrassoulis, G. Panaras, E. Giannakopoulos, S. Papaefthimiou, Green roofs as a nature-based solution for improving urban sustainability: progress and perspectives, Renew. Sustain. Energy Rev. 180 (2023) 113306, https://doi.org/10.1016/J.RSER.2023.113306.

[7] M.M. Delgado-Serrano, K. Melichová, I. Mac Fadden, C. Cruz-Piedrahita, Perception of green spaces' role in enhancing mental health and mental well-being in small and medium-sized cities, Land Use Policy 139 (2024) 107087, https://doi.org/10.1016/J.LANDUSEPOL.2024.107087.

[8] Y. Bai, R. Wang, L. Yang, Y. Ling, M. Cao, The impacts of visible green spaces on the mental well-being of university students, Appl. Spat. Anal. Policy. 17 (2024) 1105–1127, https://doi.org/10.1007/S12061-024-09578-7.

[9] T.P. Pasanen, M.P. White, L.R. Elliott, M. van den Bosch, G.N. Bratman, A. Ojala, K. Korpela, L.E. Fleming, Urban green space and mental health among people living alone: the mediating roles of relational and collective restoration in an 18-country sample, Environ Res 232 (2023) 116324, https://doi.org/10.1016/J.ENVRES.2023.116324.

[10] M. Loutou, M. Hajjaji, Clayey wastes-based lightweight aggregates: heating transformations and physical/mechanical properties, Appl. Clay Sci. 150 (2017) 56–62, https://doi.org/10.1016/J.CLAY.2017.09.011.

[11] R. Liu, R. Coffman, Lightweight aggregate made from dredged material in green roof construction for stormwater management, Materials (Basel) 9 (2016) 611, https://doi.org/10.3390/MA9080611.

[12] R. Mlih, F. Bydalek, E. Klumpp, N. Yaghi, R. Bol, J. Wenk, Light-expanded clay aggregate (LECA) as a substrate in constructed wetlands – A review, Ecol. Eng. 148 (2020) 105783, https://doi.org/10.1016/J.ECOLENG.2020.105783.

[13] M. Kazemi, L. Courard, S. Attia, Water permeability, water retention capacity, and thermal resistance of green roof layers made with recycled and artificial aggregates, Build. Environ. 227 (2023) 109776, https://doi.org/10.1016/J.BUILDENV.2022.109776.

[14] A.M. Rashad, Lightweight expanded clay aggregate as a building material – An overview, Constr. Build. Mater. 170 (2018) 757–775, https://doi.org/10.1016/J.CONBUILDMAT.2018.03.009.

[15] B. Ayati, V. Fernández-Mas, D. Newport, C. Cheeseman, Use of clay in the manufacture of lightweight aggregate, Constr. Build. Mater. 162 (2018) 124–131, https://doi.org/10.1016/J.CONBUILDMAT.2017.12.018.

[16] M. Dondi, P. Cappelletti, M. D'Amore, R. de Gennaro, S.F. Graziano, A. Langella, M. Raimondo, C. Zanelli, Lightweight aggregates from waste materials: reappraisal of expansion behavior and prediction schemes for bloating, Constr. Build. Mater. 127 (2016) 394–409, https://doi.org/10.1016/J.CONBUILDMAT.2016.09.111.

[17] N. Singh, J. Raza, F. Colangelo, I. Farina, Advancements in Lightweight Artificial Aggregates: typologies, Compositions, Applications, and Prospects for the Future, Sustainability 16 (2024) 9329, https://doi.org/10.3390/SU16219329.

[18] A. Stempkowska, T. Gawenda, Artificial lightweight aggregate made from alternative and waste raw materials, hardened using the hybrid method, Sci. Rep. 14 (2024) 1–19, https://doi.org/10.1038/s41598-024-67454-3.

[19] X. Xiong, Z. Wu, P. Jiang, M. Lai, G. Cheng, A novel method for preparing lightweight and high-strength ceramisite coarse aggregates from solid waste materials, Materials (Basel) 17 (2024) 2613, https://doi.org/10.3390/MA17112613.

[20] F. Andreola, A. Borghi, S. Pedrazzi, G. Allesina, P. Tartarini, I. Lancellotti, L. Barbieri, Spent coffee grounds in the production of lightweight clay ceramic aggregates in view of urban and agricultural sustainable development, Materials (Basel) 12 (2019) 3581, https://doi.org/10.3390/MA12213581.

[21] C. Martínez-García, F. Andreola, I. Lancellotti, R.D. Farías, M.T. Cotes-Palomino, L. Barbieri, Cleaner design and production of lightweight aggregates (LWAs) to use in agronomic application, Appl. Sci. 11 (2021) 800, https://doi.org/10.3390/APP11020800.

[22] S. Barbi, P. Barbieri, F. Andreola, I. Lancellotti, L. Barbieri, M. Montorsi, Preliminary study on sustainable NPK slow-release fertilizers based on byproducts and leftovers: a design-of-experiment approach, ACS Omega 5 (2020) 27154–27163, https://doi.org/10.1021/ACSOMEGA.0C03082/ASSET/IMAGES/MEDIUM/AO0C03082_M001.GIF.

[23] D. Ronga, M. Parisi, L. Barbieri, I. Lancellotti, F. Andreola, C. Bignami, Valorization of spent coffee grounds, biochar and other residues to produce lightweight clay ceramic aggregates suitable for nursery grapevine production, Horticulturae 6 (2020) 58, https://doi.org/10.3390/HORTICULTURAE6040058.

[24] ASTM C20, Standard Test Methods for Apparent Porosity, Water Absorption, Apparent Specific Gravity, and Bulk Density of Burned Refractory Brick and Shapes by Boiling Water, ASTM International, West Conshohocken, PA, USA, 2022.

[25] Notification of the Ministry of Agriculture and Cooperatives of Thailand; Re. Prescribing the Method of Analysis of Chemical fertilizers B.E. 2559. https://www.doa.go.th/ard/wp-content/uploads/2019/11/FEMOA13.pdf (accessed 3 February 2025).

[26] J. Carneiro, D.M. Tobaldi, W. Hajjaji, M.N. Capela, R.M. Novais, M.P. Seabra, J. A. Labrincha, Red mud as a substitute coloring agent for the hematite pigment, Ceram. Int. 44 (2018) 4211–4219, https://doi.org/10.1016/J.CERAMINT.2017.11.225.

[27] Y. Cheng, J. Xing, C. Bu, J. Zhang, G. Piao, Y. Huang, H. Xie, X. Wang, Dehydroxylation and structural distortion of kaolinite as a high-temperature sorbent in the furnace, Minerals 9 (2019) 587, https://doi.org/10.3390/MIN9100587.

[28] M. Abubakar, A. Muthuraja, D.K. Rajak, N. Ahmad, C.I. Pruncu, L. Lamberti, A. Kumar, Influence of Firing Temperature on the Physical, Thermal and Microstructural Properties of Kankara Kaolin Clay: a Preliminary Investigation, Materials (Basel) 13 (2020) 1872, https://doi.org/10.3390/MA13081872.

[29] M.I. Aoda, A.J.M. Smucker, S.S. Majeed, H.A. Mohammed, F.H. Al-Sahaf, G. P. Robertson, Novel root zone soil water retention improves production with half the water in arid sands, Agron. J. 113 (2021) 2398–2406, https://doi.org/10.1002/agj2.20648.

[30] Interaction of Perlite with Fertilizer Nutrients in Different Soil Types, 2025. https://www.perlite.org/wp-content/uploads/2024/11/Perlite-and-Fertilizer-Nutrients.pdf. accessed April 21.

[31] G.K. Kome, R.K. Enang, F.O. Tabi, B.P.K. Yerima, G.K. Kome, R.K. Enang, F.O. Tabi, B.P.K. Yerima, Influence of Clay Minerals on Some Soil Fertility Attributes: a Review, Open J. Soil Sci. 9 (2019) 155–188, https://doi.org/10.4236/OJSS.2019.99010.

[32] T. Nyi, V. Philip, M.I.B.H. Bujang, K. Ra, B. Irianto, P. Sengxua, N. Sipaseuth, A. A. Harirah, B. Bin Jantan, S.M. Salguero, P. Meunchang, V.M. Quyet, N.Q. Hai, P. Moody, T.E. Jäkel, W. Soda, ASEAN Guidelines on soil and nutrient management, 1st ed., Deutsche Gesellschaft für Internationale Zusammenarbeit (GIZ) GmbH, Germany, 2017 [Online ebook]. ISBN: 978-616-445-746-1.

[33] Notification of Thai National Committee on Agricultural Commodity and Food Standards, Subject: thai Agricultural Commodity and Food Standards: compost (TAS 9503-2005). https://faolex.fao.org/docs/pdf/tha201747.pdf. (accessed 21 February 2024).

Author biography

Name	Miss Panadda Rungrueng
Date of birth	13 October 1999
Address	2 Moo.7, Thawi Watthana Subdistrict, Sai noi District, Nonthaburi Province, 11150, Thailand
Education	(2022) Bachelor of Science in Applied Physics GPA 3.34 King Mongkut's Institute of Technology Ladkrabang (KMITL)
Scholarship	Master's Degree Scholarship supported by the Research Fund of King Mongkut's Institute of Technology Ladkrabang (KMITL)

Academic Publication

1. **Rungrueng, P.**, Hankoy, M., Kitiwan, M., Keawprak, N., & Tunthawiroon, P. (2025). *Fabrication and characterization of lightweight aggregates with expanded perlite and NPK nutrient incorporation*. **Open Ceramics**, 22, 100790. https://doi.org/10.1016/j.oceram.2025.100790